Review Article | Vol. 11, No. 4 / 1 April 2020 / Biomedical Optics Express 2017

Biomedical Optics EXPRESS

Label-free optical imaging in developmental biology [Invited]

SHANG WANG,[1] IRINA V. LARINA,[2] AND KIRILL V. LARIN[2,3,*]

[1]Department of Biomedical Engineering, Stevens Institute of Technology, 1 Castle Point Terrace, Hoboken, NJ 07030, USA
[2]Department of Molecular Physiology and Biophysics, Baylor College of Medicine, 1 Baylor Plaza, Houston, TX 77030, USA
[3]Department of Biomedical Engineering, University of Houston, 3605 Cullen Boulevard, Houston, TX 77204, USA
*klarin@uh.edu

Abstract: Application of optical imaging in developmental biology marks an exciting frontier in biomedical optics. Optical resolution and imaging depth allow for investigation of growing embryos at subcellular, cellular, and whole organism levels, while the complexity and variety of embryonic processes set multiple challenges stimulating the development of various live dynamic embryonic imaging approaches. Among other optical methods, label-free optical techniques attract an increasing interest as they allow investigation of developmental mechanisms without application of exogenous markers or fluorescent reporters. There has been a boost in development of label-free optical imaging techniques for studying embryonic development in animal models over the last decade, which revealed new information about early development and created new areas for investigation. Here, we review the recent progress in label-free optical embryonic imaging, discuss specific applications, and comment on future developments at the interface of photonics, engineering, and developmental biology.

1. Introduction

Optical imaging plays an essential role in uncovering mysteries in the early development of a new life [1–3], enabling understanding of organism formation, inspiring strategies for tissue regeneration, and providing insights into better management of congenital defects and embryonic failures. Developmental biologists have been challenging the biomedical optics community with the requirements for higher-resolution, deeper-penetration, live, dynamic, and faster imaging. Optical imaging, with a noninvasive and high-resolution nature, as well as a live imaging capability, has been responding well to such requirements. Questions in developmental biology stimulated multiple waves of optical revolution, while advancements in optical imaging played as a major factor driving discoveries in development [4–8].

Nature grants a variety of contrast mechanisms from the interaction of light with tissues and cells, which are well utilized for imaging. On one side, fluorescence is the most widely used contrast mechanism to probe targeted cellular and molecular components in embryonic tissues [9,10]. With the continuously expanding molecular genetic tools, fluorescence labeling is becoming easier, faster, more specific, and covering an increasingly broader range of model organisms [10–12]. On the other side, the employment of endogenous optical contrasts enables label-free optical imaging that addresses the intrinsic limitations of fluorescence imaging, such as photobleaching and phototoxicity [13,14], thus eliminating a major restriction in achieving high temporal resolution and long duration for imaging the dynamic developmental processes. These endogenous optical contrasts come from various photon-tissue interactions, revealing anatomical, morphological, mechanical, molecular, and functional information of the embryonic development [15–18]. As a result of such powerful capabilities, the past decade marked a surge in

#381359 https://doi.org/10.1364/BOE.381359
Journal © 2020 Received 23 Oct 2019; revised 30 Jan 2020; accepted 25 Feb 2020; published 13 Mar 2020

Biomedical Optics EXPRESS

the development of label-free optical imaging techniques in application to embryology, creating new exciting areas for investigations.

Here we attempt to review recent progress in label-free optical imaging of embryonic development. Particularly, we highlight how contrast mechanisms and imaging capabilities of each technique are advantageous for specific applications in embryonic analysis, with the goal to stimulate new ideas and developments at the interface of photonics, engineering, and developmental biology. As quantitative biology is becoming prevalent in life science, quantitative assessment achieved from non-labeling optical imaging is emphasized throughout the article. With this review, we strive to provide a useful reference of optical techniques for developmental biologists and aim to stimulate the application-driven development of advanced optical imaging methods from the biomedical optics community. By achieving these two goals, it is our hope that this article could contribute to inspiring more interdisciplinary collaborations for achieving an even faster and greater advancements in label-free optical imaging.

Recently, optical and optoacoustic (photoacoustic) imaging techniques for developmental biology was reviewed by Ripoll *et al.* [3], where the systematic discussion largely focuses on the imaging depth, speed and resolution – the three most important characteristics of the imaging methods. Different from this thorough review, we primarily focus on the connections between the fundamental contrast, imaging capability, and corresponding applications in developmental biology, highlighting indispensable features of non-labelling optical imaging as a complement to fluorescence-based techniques, thus to assist the match of specific challenges in embryology to the latest technological advances in biophotonic imaging. This article is structured based on two forms of light-tissue interactions utilized by label-free optical imaging methods: scattering and absorption. Under each category, individual imaging techniques and their applications are reviewed, which is summarized in Table 1. The major trends of this area, comparisons between the non-labeling methods and their complementary features to fluorescence imaging, as well as

Table 1. Label-free optical techniques in embryonic imaging.

Technique	Scale of Resolution	Scale of Depth	Contrast	Applications
OCT	Microns to Ten Microns	Millimeters	Refractive Index Mismatch; Speckle Variance; Doppler; Strain and Shear Stress	Tissue Structure; Vasculature; Blood Circulation; Biomechanics
OCM	Microns	Hundred Microns	Refractive Index Mismatch	Cell Structure; Tissue Structure
RM	Submicron to Microns	Hundred Microns	Raman Scattering	Biomolecule
BM	Submicron to Microns	Hundred Microns	Brillouin Scattering	Biomechanics
SHGM	Submicron to Microns	Hundred Microns	Ordered Non-Centrosymmetric Molecular Structure	Biomolecule; Tissue Structure
THGM	Submicron to Microns	Hundred Microns	Refractive Index Mismatch	Cell Structure; Blood Circulation
OPT	Microns to Ten Microns	Millimeters to Ten Millimeters	Absorption	Tissue Structure
PACT	Ten Microns to Hundred Microns	Ten Millimeters	Absorption	Vasculature; Oxygen Saturation
PAM	Microns to Ten Microns	Millimeters	Absorption	Vasculature
QPI	Submicron to Microns	Hundred Microns	Optical Path Length	Cell Structure

OCT: optical coherence tomography; OCM: optical coherence microscopy; RM: Raman microscopy; BM: Brillouin microscopy; SHGM: second harmonic generation microscopy; THGM: third harmonic generation microscopy; OPT: optical projection tomography; PACT: photoacoustic computed tomography; PAM: photoacoustic microscopy; QPI: quantitative phase imaging.

Biomedical Optics EXPRESS

the potential in addressing open questions in developmental biology are provided in the Outlook and Summary at the end of the manuscript.

2. Scattering-based techniques

2.1. Optical coherence tomography and microscopy

Introduced in 1991, optical coherence tomography (OCT) is a low-coherence imaging modality based on interferometric detection of backscattered light from tissue [19]. In general, OCT has a millimeter-level imaging depth with a micro-scale spatial resolution in 3D [20]. This unique imaging scale fits well in the gap between confocal and high-frequency ultrasound, thus providing unprecedented visualizations of early and mid-stage embryos from small animal models [21,22]. In 1996, five years after its invention, OCT was first applied to image the morphology and anatomy in frog and zebrafish embryos both *in vitro* and *in vivo*, resolving critical structures, such as the eye and brain [23,24]. Since then, OCT for embryonic imaging has been rapidly developing and evolving with a number of groups continuously pushing the limit of what information OCT can reveal in a broad range of animal models [25–36].

By capturing low-coherence interference between the backscattered light from the sample and the reflected light from the reference arm, the 1D depth-resolved OCT A-scan can be achieved by either directly mapping the optical intensity (time-domain OCT) or performing an inverse Fourier transform of the spectrally-resolved interference fringes (Fourier-domain OCT) [37]. With a 2D transverse scan of the imaging beam, the reconstructed 3D OCT intensity signals reveal the mapping of the refractive index mismatch inside the tissue, providing 3D imaging of tissue structures. As such, structural OCT imaging depicts the anatomical and morphological information from the embryos, including the eye, brain, heart, and limbs [30,38,39]. The millimeter-level imaging depth of OCT limits the access to structures inside the large-size embryo, while the recent development of rotational imaging OCT overcame this limitation by integration of multiple angles of OCT imaging [40]. The micro-scale resolution of OCT enables comparable visualizations with traditional histology [23–25,41], but features a number of appealing advantages, including a rapid imaging, no requirement of sample processing, a direct volumetric reconstruction, and most importantly, the feasibility of live dynamic assessment.

Dynamic structural OCT imaging has been a major approach to understand the embryonic cardiac activities. Depth-resolved B-scan imaging can easily achieve a frame rate sufficient to capture the dynamics of a beating heart at particular planes [26,27,42]. As a traditional OCT imaging speed is not sufficient for directly capturing the beating heart volumetrically, a number of approaches have been developed for reconstruction of a high-quality visualization of 3D cardiodynamics. These are generally achieved through sequential acquisition of 2D time lapses at different positions of the heart with a spatial step, and post-acquisitional synchronization of the time lapses to the same phase of the heartbeat cycle. For direct synchronization of the time lapses, the heart rate can be actively controlled by external pacing [43], or a secondary Doppler-based system could be utilized to passively acquire a signal from the heart beat as a reference for synchronization [29,44]. A number of post-processing algorithms for synchronization without external gating have also been developed [45–49]. Specifically, 2D time lapses covering one heartbeat cycle are synchronized to their neighbors separated by a small distance recursively from one imaging plane to the next based only on the imaging data itself to produce a 4D (3D + time) reconstruction of the beating heart with a volume rate equivalent to the B-scan acquisition rate [18,50]. A continuous effort has also been made to develop ultrahigh-speed OCT imaging systems for direct volumetric imaging of the embryonic beating heart [51–53], with the volume rates ranging from 10-20 Hz [51,52] to the most recent 43 Hz achieved through a 1.5 MHz A-scan rate [53]. These methods feature efficient phenotypic analyses and prevent possible errors induced from the sophisticated synchronization approaches, however requiring faster laser sources, which

Biomedical Optics EXPRESS

are still limited on the market. A notable application of 4D OCT cardiodynamic imaging is for phenotypic assessment of relevant genetic mutations associated with congenital heart defects in mice. For example, Lopez III *et al*. identified a cardiac looping defect in the Wdr19 mutant mice using 4D OCT structural imaging [50].

Taking advantage of the unique imaging scale, the dynamic structural OCT imaging has also been employed to investigate the cranial neural tube closure process in the mouse model [54]. With time-lapse imaging over 16 hours duration, a button-like closure in the midbrain region was observed as a distinct process from the zipper-like closure in the hindbrain region, as shown in Fig. 1, marking an interesting phenomenon during the central nervous system morphogenesis [54]. Particularly, OCT volumetric imaging enabled convenient and accurate measurements of the 3D distance between the neural folds over time, leading to a quantitative assessment of the closure dynamics and a characterization of the neural tube defect in the mutant mouse model [54]. As the developmental process involves numerous morphogenetic changes that are critical for successful establishment of different organs, similar time-lapse quantitative OCT structural analysis can be applied to study such processes during normal development and investigate the effects of genetic mutations and epigenetic factors.

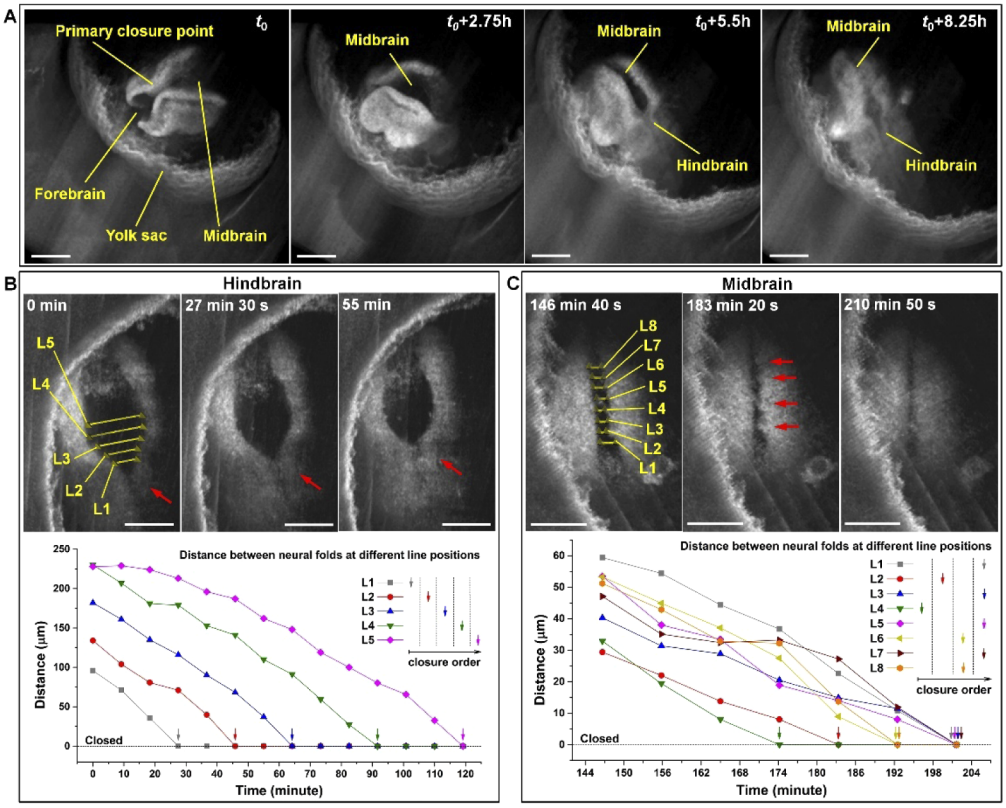

Fig. 1. Dynamic structural OCT imaging of the cranial neural tube closure in the mouse embryo. (A) Representative frames from 3D OCT time-lapse showing the closure process while the embryo is turning. (B) Zipper-like closure of neural tube at the hindbrain region with quantitative analysis. The red arrows point at the site where zipper-like closure occurs. (C) Button-like closure of neural tube at the midbrain region with quantitative analysis. The red arrows point at the sites where button-like closure occurs. Scale bars are (A) 300 μm and (B, C) 200 μm. Reproduced from [54].

Biomedical Optics EXPRESS

In addition to structural OCT imaging, functional OCT methods with novel contrast mechanisms have enabled advanced analysis of the functional aspects of embryos. These primarily include vasculature imaging with OCT angiography, blood flow imaging with Doppler OCT, and biomechanical assessment with OCT-based elastography and shear stress mapping.

Angiography with OCT is achieved through post-processing the changes of OCT intensity (speckle) or phase induced by the movement of circulating blood cells [55]. Well resolving the vasculature network of the embryos, OCT angiography is a major alternative approach to fluorescence-based imaging for functional vasculogenesis analysis [56,57]. Notably, with ultrahigh-speed imaging, the OCT angiographic analysis can be performed across multiple volumes, leading to time-lapse vasculature imaging [53]. Recently, this type of cross-volume analyses has resulted in 4D dynamic angiography of the beating mouse embryonic heart [58], allowing for advanced cardiac blood volume segmentation over the entire heartbeat cycle, which is significant for numerical modeling of the early heart biomechanics.

Doppler OCT utilizes the OCT phase signal to resolve the continuous movement of scatterers and to quantitatively measure their moving velocity [59]. First applied to embryonic imaging in 1997 [60], Doppler OCT provides robust 4D high-resolution analyses of blood flows in the embryo [18], as shown in Fig. 2. Major applications focus on flow measurements in the vasculature [28,61–63] and the beating heart [28,53,60,64,65], featuring dynamic assessment with a high spatiotemporal resolvability. Among these, 4D imaging of cardiac hemodynamics generates unprecedented visualizations [44,66]. Also, together with the analysis of cardiac wall motions, OCT hemodynamic imaging of the embryonic heart enables the understanding of how an early tubular heart pumps blood [18], revealing the biomechanics of cardiogenesis [67]. Particularly, retrograde flows in the valveless heart were observed and assessed at different locations [18,35]. The retrograde flow is recognized as an interesting mechanotransduction stimulus, deserving thorough further investigations for its specific role in endocardial cushion development and proper valve formation. Additionally, Doppler OCT imaging has been used to study altered hemodynamics introduced by different manipulations of the embryonic heart [35,68,69], which could contribute to an improved understanding of congenital heart diseases in relation to biomechanical alterations.

Biomechanical OCT imaging of the embryo has largely focused on the heart, including both elasticity assessment [34,70–72] and shear stress analysis [63,66,67,73–75]. High-resolution imaging and measurement of elasticity with OCT is an emerging area that can potentially bring a novel mechanical understanding of tissues and cells at a new scale which was previously not available [76,77]. OCT-based embryonic heart elastography primarily relies on contraction-induced strain as the contrast mechanism. Specifically, strain is measured as the change of the heart wall thickness that is inversely related to the tissue stiffness [34]. As the contractile force or pressure applied to the heart wall during pumping is unmeasurable and possibly has time-dependent and cross-sample variations, strain-related measurements remain qualitative with analyses mainly focused within an individual heart. New methods able to probe the pressure on the cardiac wall tissue would be required to combine with OCT for a quantitative elastography. In addition to the strain-based contrast, the pulse wave propagation on the embryonic outflow tract has been resolved and the velocity can be measured [53,78], which could potentially be useful to estimate the mechanical property of the outflow tract [79]. An alternative promising label-free method for embryonic mechanobiology, which is based on the analysis of photon-phonon interaction, is discussed in Section 2.3. Measuring the heart wall shear stress induced by laminar blood flows is achieved through spatial analyses of flow velocity over the heart tube cross-section [63,66]. Notably, 4D mapping of shear stress in the quail embryonic heart was achieved by Peterson *et al.* [73], which provides dynamic visualizations and understanding of spatiotemporal variations of shear force applied to the beating embryonic heart. Computational fluid dynamics were also employed to produce mapping of the heart wall shear stress [67,75]. OCT-based shear

Biomedical Optics EXPRESS

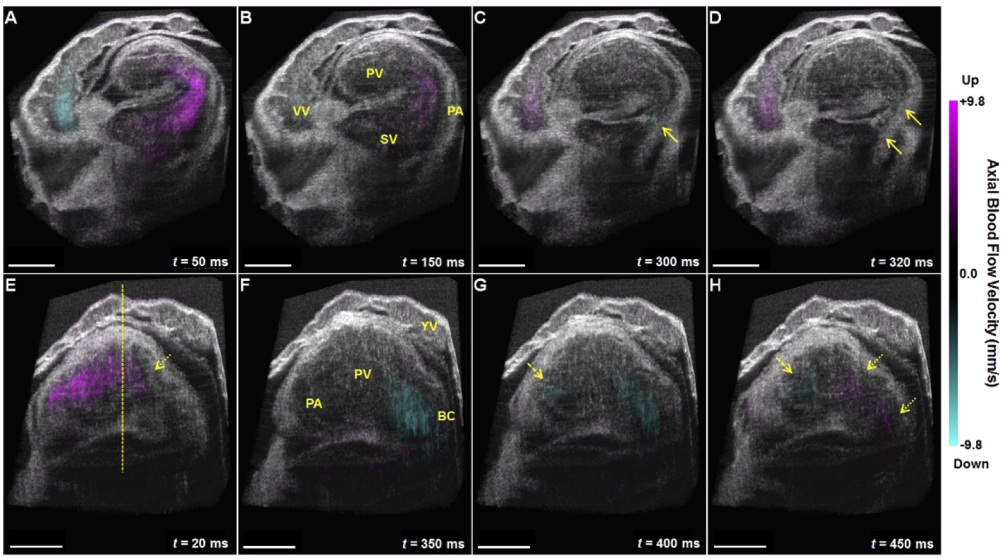

Fig. 2. Doppler 4D OCT imaging of cardiac hemodynamics in the mouse embryo at embryonic day 9.0. (A-D) Cross-sectional visualizations of the sinus venosus, primitive atrium, and vitelline vein at different time points of cardiac cycle. (E-H) Cross-sectional visualizations of the primitive ventricle and bulbus cordis at different time points of cardiac cycle. Solid arrows point at retrograde flows in the primitive atrium. Dashed arrows point at retrograde flows in the atrioventricular region. Dotted arrows point at retrograde flows in the bulbus cordis and the bulboventricular region. The dashed line in (E) shows the location that has the highest axial position. YV: yolk sac vessel; VV: vitelline vein; SV: sinus venosus; PA: primitive atrium; PV: primitive ventricle; BC: bulbus cordis. Scale bars are 200 μm. Reproduced from [18].

stress analysis has been utilized in a number of studies to investigate the hemodynamic changes of the embryonic heart during development as well as in response to a variety of stimulations and manipulations simulating the congenital heart defects [68,80–83].

Optical coherence microscopy (OCM), as a combination of OCT and confocal microscopy, achieves an improved transverse resolution with a high numerical aperture objective [84]. OCM provides a superior spatial resolvability with a 3D resolution reaching 1-2 μm while maintains an imaging depth of ~0.5 mm [85]. As such, for embryonic imaging, OCM is mainly utilized to probe the preimplantation development [85,86]. Specifically, the first division process of the mouse zygote can be clearly visualized *in vitro* with time-lapse OCM imaging, which includes the very detailed dynamics of nuclei [85]. Recently, OCM imaging of preimplantation embryos has also been achieved *in vivo* inside the mouse oviduct, promising for monitoring the mammalian preimplantation development in its native environment [86]. In addition, OCM imaging of the *Drosophila* embryonic heart demonstrates quantifications of the heart rate, the end systolic/diastolic diameter, and the fraction shortening [36,87]. Since OCM is based on the same contrast mechanism as OCT, functional OCM imaging, such as angiography, is possible [88], which could be potentially applied for functional embryonic imaging with an improved spatial resolution.

2.2. Raman microscopy

As a vibrational spectroscopic technique, Raman spectroscopy probes molecular information by analyzing the Raman scattering of photons by molecules, where the gain or loss of energy

Biomedical Optics EXPRESS

produces a shift of the scattered light frequency [89]. With the peaks in the spectrum identifying different molecules, the mapping of the Raman spectrum information produces microscopic imaging of the 3D distribution of specific molecules in tissue, as Raman microscopy (RM) [90]. Generally, RM achieves the spatial resolvability by an integration of Raman spectroscopy with existing microscopy techniques, such as confocal microscopy, thus allowing for depth-resolved imaging and possessing a sub-micron resolution that is limited by the optical diffraction [91]. Compared with fluorescence-based molecular imaging, RS is attractive for its label-free analysis, minimal sample preparation efforts, and the simultaneously acquired large amount of molecular composition data. These features have motivated a number of groups to utilize RM for targeted molecular information in embryos [92–94].

As a demonstration that RM provides very rich molecular information from the developing embryo, Nakamura *et al.* showed that the location and structure of the differentiated muscle and endoderm can be well identified in the whole *Ciona intestinalis* embryo over its early development [93], as shown in Fig. 3. Imaging the dynamics of lipid droplets in early-stage embryos has been a major application of RM in developmental biology, which has a demonstrated non-destructive nature that enables long-duration analysis [92]. Notably, with coherent anti-Stokes Raman scattering microscopy that has a significantly improved sensitivity and imaging speed [95], the size, number, and spatial distribution of lipid droplets can be quantitatively characterized in live

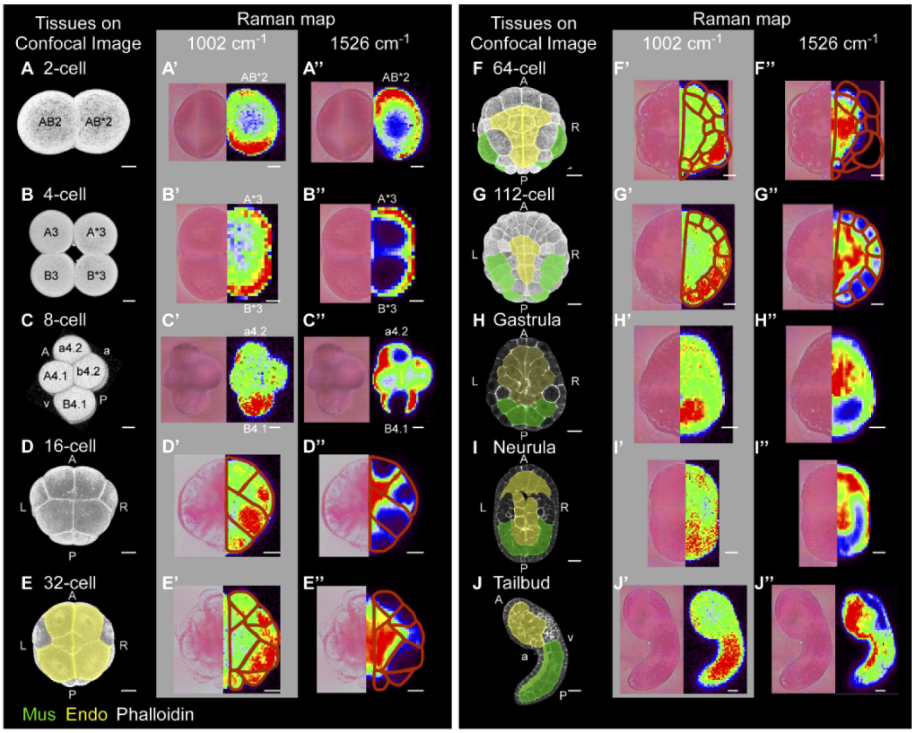

Fig. 3. RM imaging of the *Ciona intestinalis* embryo from two-cell stage to tailbud stage at the bands of 1002 cm^{-1} and 1526 cm^{-1}. (A-J) Confocal images of the embryos for references. (A'-J', A''-J'') Corresponding RM (right) images at 1002 cm^{-1} and 1526 cm^{-1}, respectively. Bright-field images (left) are provided as reference, as the embryos are bilaterally symmetrical. Red lines in D'-G' and D''-G'' outline presumed cell borders. A: anterior; P: posterior; L: left; R: right; a: animal; v: vegetal; Mus: muscle; Endo: endoderm. The colors in the images represent the Raman intensity at corresponding bands with red for the highest intensity and black for zero. Scale bars are 20 µm. Reproduced from [93].

Biomedical Optics EXPRESS

preimplantation mouse embryo without affecting the normal development [94]. A number of Raman spectroscopic analyses have recently been performed on embryos to probe the specific biomarkers for the developmental potential [17,96] and the diagnosis of stem cell differentiation [97]. The safety levels of Raman laser exposure on the early-stage mouse embryo has been systematically studied [98]. These together point to an exciting potential for a wider application of RM in the investigation of embryonic development.

2.3. Brillouin microscopy

As another nonlinear spectroscopic technique, Brillouin spectroscopy probes the Brillouin scattering of light, which is the interaction of light waves with gigahertz-frequency acoustic waves (phonons), and the resulted frequency shift of light reflects the high-frequency modulus of sample, providing the material elastic properties [99,100]. Brillouin microscopy (BM) emerges as a spectroscopic biomechanical imaging technique in 2005 [101], thanks to the significantly reduced data acquisition time to resolve the Brillouin frequency shift. Over the years after this, BM has rapidly become an attractive approach for high-resolution mechanical characterization of bulk biological samples [102] as well as sub-cellular components [103]. By employing a confocal configuration, BM can provide depth-resolved 3D micro-scale mapping of the tissue longitudinal modulus [104,105], which is highly valuable to probe the stiffness of the embryo. Particularly, the noninvasive and noncontact nature of BM is greatly desired for the delicate embryonic tissue.

The application of BM in the area of developmental biology has so far been focused on the mouse and zebrafish embryos [99,106–108]. Among these, 2D elastography was achieved from the mouse embryo at embryonic day 8.5, showing distinct mechanical properties across different organs [106]. Specifically, for the neural tube, BM imaging depicts the spatial gradient of longitudinal modulus in the dorsal-ventral direction, as shown in Fig. 4, and also suggests an increase of stiffness from the neural folds over development [107]. Recently, it has been demonstrated that BM is capable to detect the mechanical properties from distinct anatomical structures in the zebrafish embryo and also to monitor the changes of mechanical properties

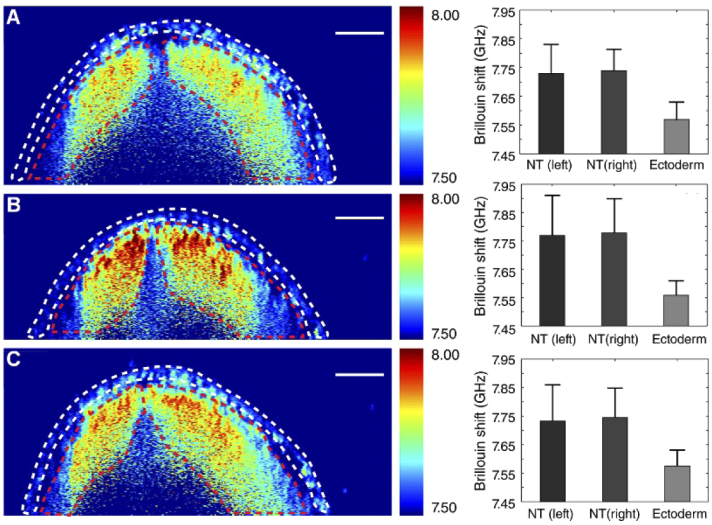

Fig. 4. BM of the neural tube at three locations from a mouse embryo at embryonic day 9.5. (A-C) BM images of the neural folds and ectoderm (left) with the corresponding quantifications of the Brillouin shift (right) showing the spatial gradient of longitudinal modulus as well as the relatively lower stiffness from the ectoderm. Scale bars are 100 μm. Reproduced from [107].

Biomedical Optics EXPRESS

during development and the recovery of spinal cord injury [108]. Compared with the widely used pipette aspiration method to measure embryonic tissue stiffness [109], BM features appealing advantages on noninvasive assessment that enables potentially repeated and longitudinal analyses.

2.4. Second and third harmonic generation microscopy

Second and third harmonic generation (SHG and THG) microscopy relies on nonlinear coherent scattering with the conversion of two or three incoming photons, respectively, to one photon of exactly doubled or tripled energy [110,111]. Unlike multiphoton fluorescence microscopy that is based on the excitation-emission mechanism, SHG and THG have the photon energy fully conserved, leading to substantially reduced photobleaching and heating. The SHG process is highly specific to the ordered non-centrosymmetric molecular structures, thus providing well defined imaging contrast for certain cellular and tissue components, such as the collagen, microtubule, and muscular myosin [112–114], which proves to be highly useful for embryonic assessment. In contrast to the high specificity of SHG, the THG process takes place at the interfaces of structures, for example, at the cell membrane, and thus probes the refractive index mismatch [111]. As a result, for embryonic imaging, THG microscopy has mainly been used to provide general structural information.

SHG microscopy was used to image the muscular architecture and the trachea system of the *Drosophila* embryo [115]. Also, interferometric SHG imaging was utilized to probe the polarity of microtubule array in the mitotic spindles of the zebrafish embryo, which suggests a new path for understanding the role of the microtubule polarity in the early developmental process [116]. Recently, SHG microscopy has also been employed for 3D imaging of the fibrillar structures in the mouse embryonic heart, showing the temporal change and spatial heterogeneity of the cardiac

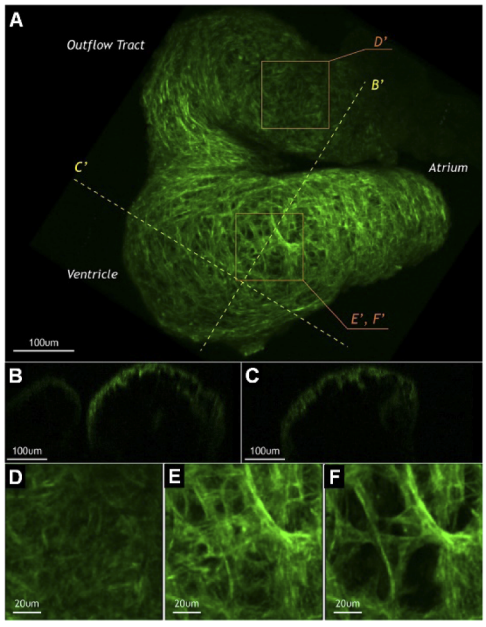

Fig. 5. SHG imaging of fibrillar structures in the mouse embryonic heart at embryonic day 8.5. (A) 3D reconstruction of SHG image of the entire heart, including the primitive atrium, primitive ventricle, and outflow tract. (B, C) Cross-sectional visualizations at the locations shown in (A). (D-F) Zoom-in visualizations at (D) the outflow track and (E, F) the ventricle from the locations labeled in (A). (F) presents 15 μm below the heart surface. Reproduced form [117].

Biomedical Optics EXPRESS

fibrillar content and organization [117], as shown in Fig. 5. Notably, quantitative SHG imaging analysis of the Mlc2a mutant mouse embryo with a reduced heart contractility indicates distinct fibrillar network [117]. As THG signals well depict the cell membranes, THG microscopy has largely focused on cell tracking, including during the early cell divisions of the *Caenorhabditis elegans* embryo [118] and for measuring blood flow velocity in the frog embryo [119].

The combination of SHG and THG imaging has been widely used for embryonic imaging, as they provide well complementary information. Specifically, for the mouse embryo from two-cell stage to blastocyst, combined SHG and THG microscopy is able to identify critical subcellular structures, such as the zona pellucida and inner cell mass [120]. Also, quantitative measurements of cell behaviors along the cell lineage of the zebrafish embryo over the first 10 cell division cycles was achieved through the combined SHG and THG imaging [121]. In particular, the intrinsic THG signals nicely highlight the cell contours, as shown in Fig. 6, which leads to high-quality observations of dynamic developmental processes [121]. For an improved spatial resolution, adaptive optics has been applied with SHG and THG microscopy for embryonic imaging [122–124], featuring high-resolution characterizations of dynamic events, such as the behavior of lipid droplets in the preimplantation mouse embryo [123].

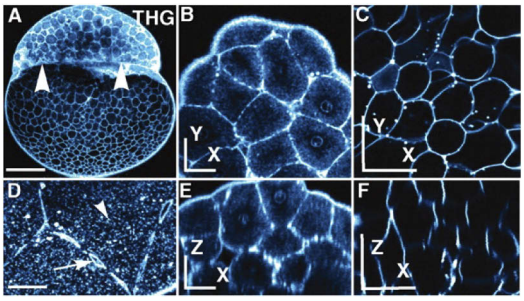

Fig. 6. THG imaging of the zebrafish embryo at 64-cell and 512-cell stages. (A) Image of 512-cell embryo with the animal pole to the top. (B, C) XY image and (E, F) XZ image of 64-cell embryo with (B, E) blastoderm cells and (C, F) yolk platelets. Light is delivered through a lens of 0.8 numerical aperture. (D) XY image of blastoderm cells. Light is delivered through a lens of 1.2 numerical aperture. Scale bars are (A) 200 µm, (B, C, E, and F) 50 µm, and (D) 30 µm. Reproduced from [121].

3. Absorption-based techniques

3.1. Optical projection tomography

In contrast to the scattering-based techniques that rely on optical sectioning for 3D reconstruction, optical projection tomography (OPT) is based on the principle of computed tomography, where a filtered back-projection algorithm is used for 3D reconstruction from the raw projection data at different orientations [125]. Invented in 2002 [6], OPT is a major embryonic imaging approach that has been widely applied in development biology, due to its distinct features of an isotropic spatial resolution down to 5 µm and an imaging depth of up to 10 mm [125]. There are two types of OPT imaging modes: transmission OPT (or bright-field OPT) where the contrast comes from light absorption of the sample, and emission OPT that resolves either autofluorescence signal or fluorescence staining of the sample [126]. While fluorescence-based OPT is an extremely useful approach to study the 3D gene expression pattern from the entire embryo [127–130], label-free absorption-based OPT finds its important applications in whole-embryo anatomical imaging primarily for understanding the organ morphology [131].

Biomedical Optics EXPRESS

Non-labeling OPT imaging has largely been focused on the mouse embryos [15,132]. Specifically, Singh *et al.* performed a systematic comparative analysis of OPT versus OCT on the embryos at embryonic days 9.5, 11.5, and 13.5, demonstrating the distinct advantages of OPT and its feasibility for whole-body imaging of large-size embryos [132]. Recently, a comparative study of OPT with micro-CT further showed that the high spatial resolution, endogenous light absorption contrast, and large field of view of OPT are well suitable for label-free imaging of the mouse embryo [15]. In particular, segmented atlas and volume quantification of 12 different major organs of the mouse embryo were achieved at embryonic day 11.5, and bone segmentation was also achieved at embryonic day 16.5, as shown in Fig. 7, demonstrating absorption-based OPT as a promising technique for quantitative morphological imaging of embryos [15]. Label-free OPT has also been utilized to image the early-stage human embryos with a focus on the brain development, indicating that many structures in the nervous system can be resolved and identified in 3D [133].

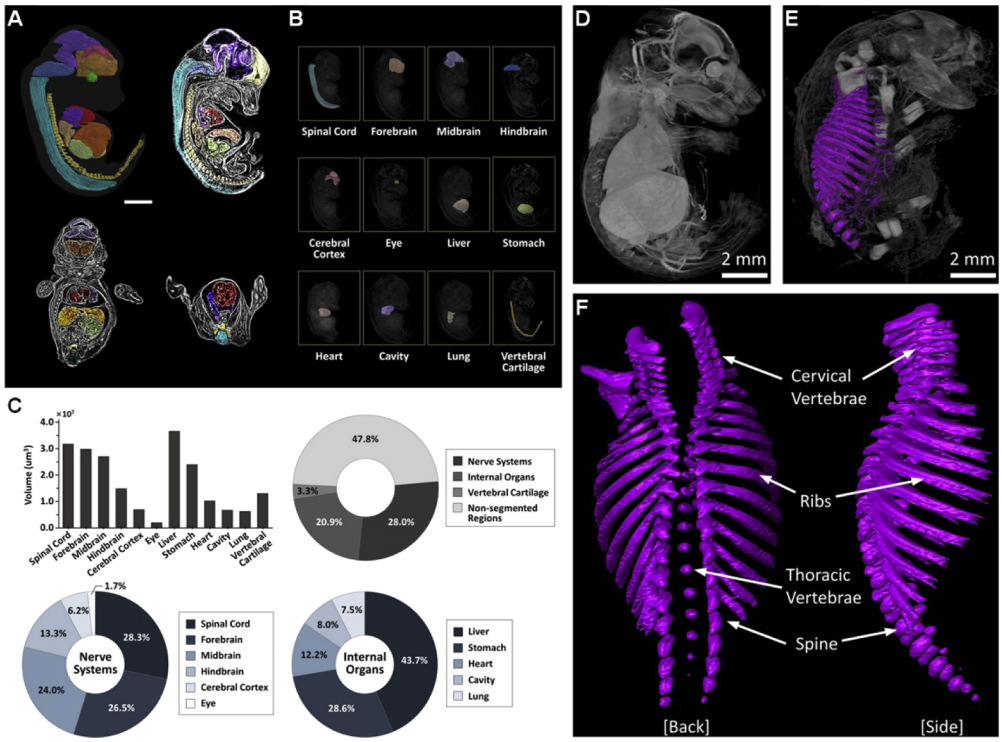

Fig. 7. Label-free OPT imaging of the mouse embryo with organ segmentation and quantitative volume measurements. (A) 3D segmented images of the mouse embryo at embryonic day 11.5. (B) Individual segmented organs highlighted from the embryo image. (C) Quantitative analysis of the organ volume. (D) 3D image of the mouse embryo at embryonic day 16.5. (E) Segmented bone highlighted from the embryo image. (F) Detailed 3D visualization of the bone structures. Scale bar in (A) is 2 mm. Reproduced from [15].

As an intrinsic requirement, scattering should be minimized for transmission OPT imaging. This can be achieved through optical clearing for large turbid samples, such as the late-stage mouse embryos [134]. Such requirement has prevented OPT from a live dynamic imaging application in the whole mouse embryo. *In vivo* label-free OPT imaging has been demonstrated for biological samples that are relatively transparent or small in size (1-2 mm), including the *Caenorhabditis elegans* [135], zebrafish [136], and early-stage *Drosophila* embryo [137]. As

Biomedical Optics EXPRESS

the number of angular projections determines the reconstruction quality, to obtain desired OPT images, the imaging speed is usually sacrificed, which leads to other limitations of not able to resolve fast movement and suffering from motion artifacts. Different methods have been developed to overcome such limitations, such as approaches to correct or compensate for the motion [135] and an iterative algorithm to reduce the required minimum number of angular projections [136]. Also, through combining *ex vivo* live tissue culture with OPT, live imaging of the early-stage mouse organogenesis has been achieved with a focus on the limb buds [138], which paves the way for *ex vivo* live 4D OPT imaging of organogenesis of the mouse embryo [139].

3.2. Photoacoustic tomography

Photoacoustic tomography (PAT) relies on the photoacoustic effect. It reconstructs the position of light absorption by probing the subsequently generated acoustic waves [140]. Due to the low scattering of acoustic waves in tissue, PAT takes advantage of the optical absorption from both the ballistic and diffusive photons, thus is able to provide label-free high-resolution imaging with an extended depth in comparison with other optical modalities [141]. Because the signal originates from the light absorption, PAT offers rich endogenous contrasts for imaging a variety of biological components by applying different optical wavelengths [142], such as hemoglobin, melanin, DNA/RNA, lipids, and water. Notably, taking advantage of the different absorption spectra of oxy- and deoxy-hemoglobin, PAT allows not only for structural imaging of vasculature and functional imaging of blood circulation, but also oxygen saturation and metabolic imaging of oxygen consumption [143]. Two implementations of PAT have been applied for embryonic imaging: photoacoustic computed tomography (PACT) and photoacoustic microscopy (PAM). PACT employs an expanded optical beam and an array of ultrasound transducers for 3D imaging with a centimeter-level imaging depth and a spatial resolution typically at tens and hundreds of microns [144]. As a microscopic imaging technique, PAM utilizes co-focused light excitation and sound detection to achieve a micro-scale spatial resolution with a millimeter-level imaging depth [145]. The feature of PAT in multi-scale and multi-contrast imaging has found exciting applications in developmental biology.

Given the superior depth of view of PACT, *in vivo* imaging of the embryo inside the pregnant mouse at embryonic day 15.5 has been achieved [146], as shown in Fig. 8. The nicely resolved embryonic vasculature network indicates the potential for powerful *in vivo* phenotypic analyses of vasculogenesis and associated pathology [146]. PACT has also been employed to image oxygen saturation from the developing embryo in the pregnant mouse *in vivo* [147]. The approach features quantitative analysis and longitudinal assessment over embryonic day 8.5-16.5 [147], which is promising for *in vivo* longitudinal functional study of mammalian embryonic development. In addition to the mouse model, integrated PACT and OCT presents *in toto* imaging of the chick embryo with complementary scattering and absorption contrasts [148].

The application of PAM in embryonic imaging mainly focused on the zebrafish model [149]. Specifically, the formation of the cardio-cerebrovascular network was well resolved by optical-resolution PAM [150], which enables the analysis of vascular phenotypes in diseased models, such as the effects of anti-angiogenic drugs on the vasculature development [151]. Continuous efforts have been made to further improve the spatial resolution of PAM [145], which demonstrates finer imaging of the zebrafish embryo with a consistent spatial resolution over the entire body [152]. Although possessing a similar imaging scale as OCT, PAM features a distinct optical absorption contrast that makes it useful for the vasculature- and melanin-related imaging applications in the embryonic development.

In addition to the hemoglobin and melanin-based contrast, other endogenous contrast agents of PAT, although have not yet been applied for embryonic imaging, offer great potentials for multi-contrast imaging at different scales. As DNA and RNA have a strong optical absorption

Biomedical Optics EXPRESS

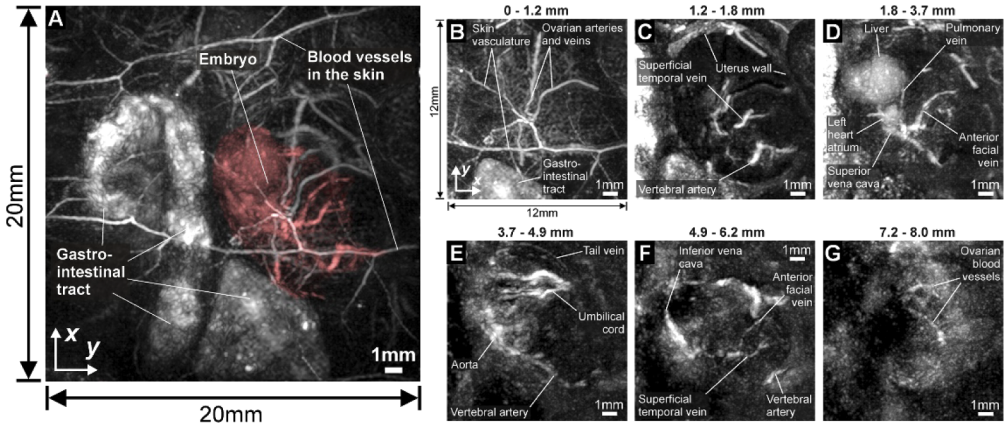

Fig. 8. *In vivo* PACT imaging of the embryo in the pregnant mouse at embryonic day 15.5. (A) Maximum intensity projection of the 3D PACT image showing the embryonic vasculature indicated in red. The red-color labeling was obtained through volume segmentation of the 3D data followed by fused color volume rendering. (B-G) PACT images at different depth ranges from (A). Reproduced from [146].

around 260 nm, with ultraviolet light, the cell nuclei can be imaged with a good contrast-to-noise ratio using PAM [153]. However, for potential live embryonic imaging, the applied laser energy and the illumination area needs to be carefully tested and optimized to avoid tissue damage caused by ultraviolet light. By utilizing near-infrared light, lipids (1210 nm and 1730 nm), water (975 nm), and collagen (1725 nm) can be imaged inside the biological tissues [154–156]. With multispectral PAT, the contrast can be further enhanced by employing several wavelengths within the corresponding absorption spectrum [157]. These contrasts in combination with the multiple imaging scales of PAT could be of great interest for studying the embryonic development of various organs, such as the heart and brain, where validations and feasibility analyses are highly anticipated.

4. Outlook and summary

Optical scattering (linear and non-linear) and absorption are two major fundamental contrast mechanisms for label-free embryonic imaging. There are optical imaging techniques based on other endogenous optical contrasts that we envision could also be useful to study questions in developmental biology. One of these is phase contrast microscopy, a label-free technique for the biological samples that weakly scatter or absorb light, such as the preimplantation embryo. Based on transmission bright-field microscopy, the phase contrast is probed through coherence light interference, resolving cellular components that are relatively transparent. Quantitative phase imaging (QPI), as an advanced phase contrast microscopic method, attracts an increasing interest for its ability of quantitatively measuring the cellular dynamics at a nanometer scale in 3D through quantifying the optical phase [158]. QPI has been applied for different types of cells with applications in understanding neural network organization [159], simultaneously assessing cell motility and growth [160], as well as measuring cell mechanics [161]. Recently, QPI has been utilized to probe the viability of *in vitro* bovine embryos by 3D label-free imaging of detailed cellular structures [162], suggesting the feasibility to study the preimplantation embryonic development.

As summarized in Table 1, similar imaging capabilities exist between the label-free imaging modalities for developmental biology. Here we want to emphasize their specific differences for particular applications. OCT and OPT both provide structural and morphological imaging of

Biomedical Optics EXPRESS

organogenesis with a resolution at micro-level. Among these, OPT achieves a higher imaging depth that is able to cover the entire large-size embryo. In contrast, OCT only probes structures that are close to the surface. However, OCT has the advantage in live dynamic imaging, which is generally not achievable by OPT due to the fixation and clearing procedures [54,132]. For imaging of vasculogenesis and angiogenesis, PAT directly relies on the optical absorption from hemoglobin and can provide volumetric reconstruction from deep inside the tissue, while OCT achieves the vasculature imaging through functional blood flow analysis with a relatively limited depth. One advantage of OCT is the capability of simultaneous imaging the vasculature together with high-resolution tissue structure [58], which is usually not feasible from PAT. For biomechanical imaging of embryonic tissues, OCT-based elastography requires proper loading to be delivered to the targeted place without damaging the embryos. For the heart, the active contractile force acts as a natural loading, enabling OCT to assess the strain and strain rate of heart wall [34]. However, for other organs or tissues, biomechanical imaging with OCT could be limited by the lack of suitable loading methods and has not been demonstrated so far. Unlike OCT, BM does not require external loading and can, therefore, be theoretically applied to any embryonic tissue from where the Brillouin scattered light can be collected. BM is an emerging technique for biomechanical imaging and has only recently been employed in a few studies for embryonic analysis [106–108], but since the significance of mechanical factors is increasingly recognized in embryonic development [163], we expect to see a rapid growth soon in the application of BM in developmental biology.

Compared with fluorescence imaging, one major advantage of label-free optical imaging is the convenience and easiness in sample preparation as complexity and unknowns still exist in fluorescence labeling of certain components, despite continuous technical advancements [164]. Also, there is no need to consider issues associated with photobleaching and phototoxicity [13,14], making it possible to achieve higher temporal resolution and higher duration for dynamic and time-lapse imaging. On the other hand, fluorescence imaging has superior contrast and is able to resolve multiple components with excellent specificity. Especially, recent advancements in next-generation light-sheet microscopy enabled larger-field-of-view, higher-resolution, and faster imaging and is promising to solve the traditional limitations in relation to fluorescence [165–167]. As such, it is expected that label-free techniques are good complementary imaging approaches for fluorescence imaging that is still the dominant imaging method in developmental biology. Combination of fluorescent and label-free imaging might provide complementary information otherwise unattainable by each individual modality [168].

It is worth to note that multiple label-free techniques can also probe fluorescence markers [127,169,170]. For example, the molecular imaging capability of PAT has shown great promise to capture fluorochromes and genetically encoded reporters at an unprecedented depth and resolution [171–174]. Thus, it might be possible to obtain both labeled and label-free imaging with a single modality, maximizing the contrast and information.

Because developmental processes are very diverse, a single type of imaging contrast can only provide limited information, and thus, multi-modal imaging approach has become a popular trend for potentially multi-contrast phenotypic analyses of embryos [175,176]. For example, OCT and spectrally encoded confocal microscopy were used together to assess the microstructure of the mouse embryonic heart [51], BM and OCT provided biomechanical and structural information of the mouse embryonic neural tube [106,107], and an integrated OCT and PAT system took advantage of the tissue structural contrast to complement the vasculature imaging [148]. Non-labeling optical imaging has been combined with ultrasonic imaging for ultrasound-guided analysis of hemoglobin oxygenation in the mouse conceptus tissues [147], as well as with fluorescence-based imaging to simultaneously probe a large amount of cellular information from the zebrafish embryos [121]. We expect to see the emergence of novel optical multi-modality approaches in the future.

Biomedical Optics EXPRESS

Integrating optical imaging with embryonic manipulation techniques is another exciting frontier of this interdisciplinary field, which would benefit from further development. Specifically, OCT-guided microinjections to the embryonic vasculature provided the opportunity to study the flow dynamics before the circulation of blood cells [42]. The integrated optogenetics/OCM system allowed for high-resolution dynamic characterization of the optogenetic control of the *Drosophila* embryonic heart [177]. Physical banding of the cardiac outflow track in chick embryos was utilized together with OCT to study possible mechanical contributions to the associated heart malformations [68,78]. Also, optical pacing was utilized to induce an increase of regurgitant flow in the chick embryonic heart, and OCT was used to image and measure the flow and the cardiac morphology, revealing cardiac cushion defects in relation to a high regurgitant flow [35]. We believe such work will inspire more ideas and efforts in developing combined imaging and manipulation tools for novel studies of embryos.

A variety of animal models have been studied by label-free optical imaging [178,179]. Embryos from certain model organisms, such as the zebrafish and *Drosophila*, require minimal preparations and maintenance for live imaging, convenient for technical development. In contrast, mammalian models, such as the mouse, require optimal embryo culture for live imaging [180]. Thus, establishing effective live culturing protocols has been a critical factor to advance live optical imaging of mouse embryos. The mouse is the only mammalian organism with well-established genetic engineering strategies to generate various disease models, including the congenital defects [181,182]. As an increasing number of mutant mice are created every day, there is a dramatic need for phenotypic imaging analyses of the created models. With the continuous advancements in culturing approaches, we foresee an increasing interest and development of high-throughput approaches for high-resolution mouse embryonic imaging.

Advancements in automatization of signal and image processing is another important aspect in label-free optical imaging of developmental processes. Sophisticated reconstruction algorithms are being developed to perform 3D visualizations in an efficient and even real-time fashion [183]. Automatization of data processing methods reducing the time and labor cost is particularly relevant for large-scale embryo phenotyping projects [184]. For applications in embryonic imaging, recently, deep-learning methods have been utilized for automatically segmenting the *Drosophila* heart in OCM images [87], which marks an exciting start for the employment of state-of-the-art data processing approaches in image analysis for understanding the mechanisms regulating embryonic development. We anticipate great expansion of various deep-learning and artificial intelligence algorithms applied to the field of optical imaging in development biology in the nearest future.

The imaging capabilities of the label-free optical techniques can provide unique approaches in addressing a number of developmental biology questions that are difficult to study with other methods. Here we discuss some examples that could be of interest to pursue. As the first organ to function, the heart undergoes dramatic morphological changes in early-stage development, which has been well revealed by scanning electron microscopy [185]; however, the underlying functional and biomechanical aspects of the morphogenesis remain to be elucidated [186]. The early-stage heart is valveless, and its pumping mechanism has historically drawn great interest [187]. Although different models were proposed, a uniform theory has yet to form, as how the tubular embryonic heart pumps blood remains as an open question. OCT provides volumetric and simultaneous imaging of cardiodynamics and hemodynamics of the early embryonic heart without labeling [18,188]. This enables quantitative analysis of the blood flow in combination with the heart wall movement, promising to provide new insights into the pumping mechanism. Notably, previous characterizations were largely performed on the zebrafish model by confocal fluorescence microscopy [189,190]. The deeper penetration depth of OCT allows for volumetric analysis of pumping with the mouse model, which would benefit from a wide range of transgenic models. Focusing on cardiac elasticity, the extracellular matrix plays an essential

Biomedical Optics EXPRESS

role in defining the stiffness of the early embryonic heart, creating the mechanical environment for the cardiomyocytes [191]. As such, in pursuit of understanding how shear and contractile forces regulate the heart stiffness and the extracellular matrix deposition during development, SHG imaging of cardiac fibrillar structures with high specificity could be useful for convenient and quantitative phenotypic analyses [117]. Abnormal development of central nervous system is the cause of another major congenital disease. Studies of the underlying mechanisms have been mainly focused on the molecular genetic level [192], while the understanding of the brain developmental process from dynamic, functional, and biomechanical aspects is largely absent. In relation to the brain morphogenesis, live 4D OPT imaging [138] can potentially be used to reveal this developmental process in *ex vivo* cultures, while time-lapse 3D OCT imaging is able to provide quantitative assessment of the neural fold dynamics in cultured live embryos [54]. For the investigation of the brain angiogenesis, 3D OCT angiography enables label-free longitudinal imaging of the embryonic vasculature *in utero* [193,194]. Neural tube closure, as the primary process for the neural tube formation, has been attracting continuous interest in developmental biology [195], and biomechanics was recently shown as an important factor in this dynamic process [196]. The integration of BM and OCT allows for simultaneous delineation of neural fold morphology and mapping of stiffness [107], which will be a powerful tool to investigate the spatiotemporal mechanical variations over the closure process. At the preimplantation stage, lipid plays an important metabolic role in the embryonic development [197]. Despite the known existence of lipids in early embryos, their specific functions remain less studied [197]. Recent work has developed methods to manipulate lipids in the embryos [198], and RM with its non-labeling nature could provide convenient and long-term assessment of the amount and spatial distribution of lipid droplets, thus to further characterize the functions of lipid in development.

In summary, we reviewed label-free optical imaging of embryonic development, discussed the various endogenous imaging contrasts in relation to particular applications, and commented on the differences between these techniques and the emerging trends in this interdisciplinary area. We hope that this review will encourage more biophotonic engineers to join the exciting area of developmental biology research and will serve as a reference for the developmental biology community while selecting the most suitable methods for their specific applications. Cross-disciplinary research is challenging but is highly rewarding; we hope this review will stimulate collaborative interactions between optical engineers and developmental biologists to expand the area of biophotonics in studying the early stages of a new life.

Funding

National Institutes of Health (R01EB027099, R01HD086765, R01HD095520, R01HD096335, R01HL146745, R21EB028409).

Acknowledgments

We would like to thank Professor Jan Laufer (Martin-Luther-Universität Halle-Wittenberg) for providing high-resolution images for Fig. 8.

Disclosures

The authors declare that there are no conflicts of interest related to this article.

References

1. *Imaging in Developmental Biology: A Laboratory Manual* (Cold Spring Harbor Laboratory Press, 2011).
2. W. Du, Y. Wang, Q. Luo, and B.-F. Liu, "Optical molecular imaging for systems biology: from molecule to organism," Anal. Bioanal. Chem. **386**(3), 444–457 (2006).
3. J. Ripoll, B. Koberstein-Schwarz, and V. Ntziachristos, "Unleashing Optics and Optoacoustics for Developmental Biology," Trends Biotechnol. **33**(11), 679–691 (2015).

Biomedical Optics EXPRESS

4. J. G. White, W. B. Amos, and M. Fordham, "An evaluation of confocal versus conventional imaging of biological structures by fluorescence light microscopy," J. Cell Biol. **105**(1), 41–48 (1987).
5. J. M. Squirrell, D. L. Wokosin, J. G. White, and B. D. Bavister, "Long-term two-photon fluorescence imaging of mammalian embryos without compromising viability," Nat. Biotechnol. **17**(8), 763–767 (1999).
6. J. Sharpe, U. Ahlgren, P. Perry, B. Hill, A. Ross, J. Hecksher-Sorensen, R. Baldock, and D. Davidson, "Optical projection tomography as a tool for 3D microscopy and gene expression studies," Science **296**(5567), 541–545 (2002).
7. R. Tomer, K. Khairy, F. Amat, and P. J. Keller, "Quantitative high-speed imaging of entire developing embryos with simultaneous multiview light-sheet microscopy," Nat. Methods **9**(7), 755–763 (2012).
8. K. McDole, L. Guignard, F. Amat, A. Berger, G. Malandain, L. A. Royer, S. C. Turaga, K. Branson, and P. J. Keller, "In Toto Imaging and Reconstruction of Post-Implantation Mouse Development at the Single-Cell Level," Cell **175**(3), 859–876.e33 (2018).
9. J. W. Lichtman and J.-A. Conchello, "Fluorescence microscopy," Nat. Methods **2**(12), 910–919 (2005).
10. M. Mavrakis, O. Pourquié, and T. Lecuit, "Lighting up developmental mechanisms: how fluorescence imaging heralded a new era," Development **137**(3), 373–387 (2010).
11. R. Yuste, "Fluorescence microscopy today," Nat. Methods **2**(12), 902–904 (2005).
12. S. Veerapathiran and T. Wohland, "Fluorescence techniques in developmental biology," J. Biosci. (New Delhi, India) **43**(3), 541–553 (2018).
13. R. A. Hoebe, C. H. Van Oven, T. W. J. Gadella, P. B. Dhonukshe, C. J. F. Van Noorden, and E. M. M. Manders, "Controlled light-exposure microscopy reduces photobleaching and phototoxicity in fluorescence live-cell imaging," Nat. Biotechnol. **25**(2), 249–253 (2007).
14. V. Magidson and A. Khodjakov, "Circumventing photodamage in live-cell microscopy," Methods Cell Biol. **114**, 545–560 (2013).
15. S. Ban, N. H. Cho, E. Min, J. K. Bae, Y. Ahn, S. Shin, S.-A. Park, Y. Lee, and W. Jung, "Label-free optical projection tomography for quantitative three-dimensional anatomy of mouse embryo," J. Biophotonics **12**, e201800481 (2019).
16. M. D. Wong, M. C. van Eede, S. Spring, S. Jevtic, J. C. Boughner, J. P. Lerch, and R. M. Henkelman, "4D atlas of the mouse embryo for precise morphological staging," Development **142**(20), 3583–3591 (2015).
17. M. Ishigaki, K. Hashimoto, H. Sato, and Y. Ozaki, "Non-destructive monitoring of mouse embryo development and its qualitative evaluation at the molecular level using Raman spectroscopy," Sci. Rep. **7**(1), 43942 (2017).
18. S. Wang, D. S. Lakomy, M. D. Garcia, A. L. Lopez III, K. V. Larin, and I. V. Larina, "Four-dimensional live imaging of hemodynamics in mammalian embryonic heart with Doppler optical coherence tomography," J. Biophotonics **9**(8), 837–847 (2016).
19. D. Huang, E. A. Swanson, C. P. Lin, J. S. Schuman, W. G. Stinson, W. Chang, M. R. Hee, T. Flotte, K. Gregory, C. A. Puliafito, and J. G. Fujimoto, "Optical coherence tomography," Science **254**(5035), 1178–1181 (1991).
20. A. F. Fercher, W. Drexler, C. K. Hitzenberger, and T. Lasser, "Optical coherence tomography - principles and applications," Rep. Prog. Phys. **66**(2), 239–303 (2003).
21. J. Men, Y. Huang, J. Solanki, X. Zeng, A. Alex, J. Jerwick, Z. Zhang, R. E. Tanzi, A. Li, and C. Zhou, "Optical Coherence Tomography for Brain Imaging and Developmental Biology," IEEE J. Sel. Top. Quantum Electron. **22**(4), 6803213 (2016).
22. R. Raghunathan, M. Singh, M. E. Dickinson, and K. V. Larin, "Optical coherence tomography for embryonic imaging: a review," J. Biomed. Opt. **21**(5), 050902 (2016).
23. S. A. Boppart, M. E. Brezinski, B. E. Bouma, G. J. Tearney, and J. G. Fujimoto, "Investigation of developing embryonic morphology using optical coherence tomography," Dev. Biol. (Amsterdam, Neth.) **177**(1), 54–63 (1996).
24. S. A. Boppart, B. E. Bouma, M. E. Brezinski, G. J. Tearney, and J. G. Fujimoto, "Imaging developing neural morphology using optical coherence tomography," J. Neurosci. Methods **70**(1), 65–72 (1996).
25. S. A. Boppart, G. J. Tearney, B. E. Bouma, J. F. Southern, M. E. Brezinski, and J. G. Fujimoto, "Noninvasive assessment of the developing Xenopus cardiovascular system using optical coherence tomography," Proc. Natl. Acad. Sci. U. S. A. **94**(9), 4256–4261 (1997).
26. T. M. Yelbuz, M. A. Choma, L. Thrane, M. L. Kirby, and J. A. Izatt, "Optical coherence tomography: a new high-resolution imaging technology to study cardiac development in chick embryos," Circulation **106**(22), 2771–2774 (2002).
27. J. Manner, L. Thrane, K. Norozi, and T. M. Yelbuz, "High-resolution in vivo imaging of the cross-sectional deformations of contracting embryonic heart loops using optical coherence tomography," Dev. Dyn. **237**(4), 953–961 (2008).
28. V. X. Yang, M. Gordon, E. Seng-Yue, S. Lo, B. Qi, J. Pekar, A. Mok, B. Wilson, and I. Vitkin, "High speed, wide velocity dynamic range Doppler optical coherence tomography (Part II): Imaging in vivo cardiac dynamics of Xenopus laevis," Opt. Express **11**(14), 1650–1658 (2003).
29. M. W. Jenkins, O. Q. Chughtai, A. N. Basavanhally, M. Watanabe, and A. M. Rollins, "In vivo gated 4D imaging of the embryonic heart using optical coherence tomography," J. Biomed. Opt. **12**(3), 030505 (2007).
30. S. H. Syed, K. V. Larin, M. E. Dickinson, and I. V. Larina, "Optical coherence tomography for high-resolution imaging of mouse development in utero," J. Biomed. Opt. **16**(4), 046004 (2011).
31. I. V. Larina, K. V. Larin, M. J. Justice, and M. E. Dickinson, "Optical Coherence Tomography for live imaging of mammalian development," Curr. Opin. Genet. Dev. **21**(5), 579–584 (2011).

Biomedical Optics EXPRESS

32. I. V. Larina, K. Furushima, M. E. Dickinson, R. R. Behringer, and K. V. Larin, "Live imaging of rat embryos with Doppler swept-source optical coherence tomography," J. Biomed. Opt. **14**(5), 050506 (2009).
33. X. Yin, A. Liu, K. L. Thornburg, R. K. Wang, and S. Rugonyi, "Extracting cardiac shapes and motion of the chick embryo heart outflow tract from four-dimensional optical coherence tomography images," J. Biomed. Opt. **17**(9), 0960051 (2012).
34. J. Yoo, I. V. Larina, K. V. Larin, M. E. Dickinson, and M. Liebling, "Increasing the field-of-view of dynamic cardiac OCT via post-acquisition mosaicing without affecting frame-rate or spatial resolution," Biomed. Opt. Express **2**(9), 2614–2622 (2011).
35. S. M. Ford, M. T. McPheeters, Y. T. Wang, P. Ma, S. Gu, J. Strainic, C. Snyder, A. M. Rollins, M. Watanabe, and M. W. Jenkins, "Increased regurgitant flow causes endocardial cushion defects in an avian embryonic model of congenital heart disease," Congenit Heart Dis **12**(3), 322–331 (2017).
36. A. Alex, A. Li, X. Zeng, R. E. Tate, M. L. McKee, D. E. Capen, Z. Zhang, R. E. Tanzi, and C. Zhou, "A Circadian Clock Gene, Cry, Affects Heart Morphogenesis and Function in Drosophila as Revealed by Optical Coherence Microscopy," PLoS One **10**(9), e0137236 (2015).
37. J. A. Izatt and M. A. Choma, "Theory of Optical Coherence Tomography," in *Optical Coherence Tomography: Technology and Applications*, W. Drexler and J. G. Fujimoto, eds. (Springer Berlin Heidelberg, Berlin, Heidelberg, 2008), pp. 47–72.
38. I. V. Larina, S. H. Syed, N. Sudheendran, P. A. Overbeek, M. E. Dickinson, and K. V. Larin, "Optical coherence tomography for live phenotypic analysis of embryonic ocular structures in mouse models," J. Biomed. Opt. **17**(8), 081410 (2012).
39. N. Sudheendran, S. Bake, R. C. Miranda, and K. V. Larin, "Comparative assessments of the effects of alcohol exposure on fetal brain development using optical coherence tomography and ultrasound imaging," J. Biomed. Opt. **18**(2), 020506 (2013).
40. C. Wu, N. Sudheendran, M. Singh, I. V. Larina, M. E. Dickinson, and K. V. Larin, "Rotational imaging optical coherence tomography for full-body mouse embryonic imaging," J. Biomed. Opt. **21**(2), 026002 (2016).
41. M. W. Jenkins, P. Patel, H. Deng, M. M. Montano, M. Watanabe, and A. M. Rollins, "Phenotyping transgenic embryonic murine hearts using optical coherence tomography," Appl. Opt. **46**(10), 1776–1781 (2007).
42. S. H. Syed, A. J. Coughlin, M. D. Garcia, S. Wang, J. L. West, K. V. Larin, and I. V. Larina, "Optical coherence tomography guided microinjections in live mouse embryos: high-resolution targeted manipulation for mouse embryonic research," J. Biomed. Opt. **20**(07), 1–7 (2015).
43. M. W. Jenkins, F. Rothenberg, D. Roy, V. P. Nikolski, Z. Hu, M. Watanabe, D. L. Wilson, I. R. Efimov, and A. M. Rollins, "4D embryonic cardiography using gated optical coherence tomography," Opt. Express **14**(2), 736–748 (2006).
44. A. Mariampillai, B. A. Standish, N. R. Munce, C. Randall, G. Liu, J. Y. Jiang, A. E. Cable, I. A. Vitkin, and V. X. Yang, "Doppler optical cardiogram gated 2D color flow imaging at 1000 fps and 4D in vivo visualization of embryonic heart at 45 fps on a swept source OCT system," Opt. Express **15**(4), 1627–1638 (2007).
45. M. Gargesha, M. W. Jenkins, D. L. Wilson, and A. M. Rollins, "High temporal resolution OCT using image-based retrospective gating," Opt. Express **17**(13), 10786–10799 (2009).
46. A. Liu, R. Wang, K. L. Thornburg, and S. Rugonyi, "Efficient postacquisition synchronization of 4-D nongated cardiac images obtained from optical coherence tomography: application to 4-D reconstruction of the chick embryonic heart," J. Biomed. Opt. **14**(4), 044020 (2009).
47. C. M. Happel, J. Thommes, L. Thrane, J. Manner, T. Ortmaier, B. Heimann, and T. M. Yelbuz, "Rotationally acquired four-dimensional optical coherence tomography of embryonic chick hearts using retrospective gating on the common central A-scan," J. Biomed. Opt. **16**(9), 096007 (2011).
48. I. V. Larina, K. V. Larin, M. E. Dickinson, and M. Liebling, "Sequential Turning Acquisition and Reconstruction (STAR) method for four-dimensional imaging of cyclically moving structures," Biomed. Opt. Express **3**(3), 650–660 (2012).
49. S. Bhat, I. V. Larina, K. V. Larin, M. E. Dickinson, and M. Liebling, "4D Reconstruction of the Beating Embryonic Heart From Two Orthogonal Sets of Parallel Optical Coherence Tomography Slice-Sequences," IEEE Trans. Med. Imaging **32**(3), 578–588 (2013).
50. A. L. Lopez III, S. Wang, K. V. Larin, P. A. Overbeek, and I. V. Larina, "Live four-dimensional optical coherence tomography reveals embryonic cardiac phenotype in mouse mutant," J. Biomed. Opt. **20**(9), 090501 (2015).
51. R. Yelin, D. Yelin, W. Y. Oh, S. H. Yun, C. Boudoux, B. J. Vakoc, B. E. Bouma, and G. J. Tearney, "Multimodality optical imaging of embryonic heart microstructure," J. Biomed. Opt. **12**(6), 064021 (2007).
52. M. W. Jenkins, D. C. Adler, M. Gargesha, R. Huber, F. Rothenberg, J. Belding, M. Watanabe, D. L. Wilson, J. G. Fujimoto, and A. M. Rollins, "Ultrahigh-speed optical coherence tomography imaging and visualization of the embryonic avian heart using a buffered Fourier Domain Mode Locked laser," Opt. Express **15**(10), 6251–6267 (2007).
53. S. Wang, M. Singh, A. L. Lopez 3rd, C. Wu, R. Raghunathan, A. Schill, J. Li, K. V. Larin, and I. V. Larina, "Direct four-dimensional structural and functional imaging of cardiovascular dynamics in mouse embryos with 1.5 MHz optical coherence tomography," Opt. Lett. **40**(20), 4791–4794 (2015).

Biomedical Optics EXPRESS

54. S. Wang, M. D. Garcia, A. L. Lopez 3rd, P. A. Overbeek, K. V. Larin, and I. V. Larina, "Dynamic imaging and quantitative analysis of cranial neural tube closure in the mouse embryo using optical coherence tomography," Biomed. Opt. Express **8**(1), 407–419 (2017).
55. C.-L. Chen and R. K. Wang, "Optical coherence tomography based angiography [Invited]," Biomed. Opt. Express **8**(2), 1056–1082 (2017).
56. N. Sudheendran, S. H. Syed, M. E. Dickinson, I. V. Larina, and K. V. Larin, "Speckle variance OCT imaging of the vasculature in live mammalian embryos," Laser Phys. Lett. **8**(3), 247–252 (2011).
57. P. M. Kulkarni, N. Rey-Villamizar, A. Merouane, N. Sudheendran, S. Wang, M. Garcia, I. V. Larina, B. Roysam, and K. V. Larin, "Algorithms for improved 3-D reconstruction of live mammalian embryo vasculature from optical coherence tomography data," Quant. Imaging. Med. Surg. **5**, 125–135 (2014).
58. O. A. Grishina, S. Wang, and I. V. Larina, "Speckle variance optical coherence tomography of blood flow in the beating mouse embryonic heart," J. Biophotonics **10**(5), 735–743 (2017).
59. R. A. Leitgeb, R. M. Werkmeister, C. Blatter, and L. Schmetterer, "Doppler optical coherence tomography," Prog. Retinal Eye Res. **41**, 26–43 (2014).
60. S. Yazdanfar, M. D. Kulkarni, and J. A. Izatt, "High resolution imaging of in vivo cardiac dynamics using color Doppler optical coherence tomography," Opt. Express **1**(13), 424–431 (1997).
61. I. V. Larina, S. Ivers, S. Syed, M. E. Dickinson, and K. V. Larin, "Hemodynamic measurements from individual blood cells in early mammalian embryos with Doppler swept source OCT," Opt. Lett. **34**(7), 986–988 (2009).
62. I. V. Larina, N. Sudheendran, M. Ghosn, J. Jiang, A. Cable, K. V. Larin, and M. E. Dickinson, "Live imaging of blood flow in mammalian embryos using Doppler swept-source optical coherence tomography," J. Biomed. Opt. **13**(6), 060506 (2008).
63. A. Davis, J. Izatt, and F. Rothenberg, "Quantitative Measurement of Blood Flow Dynamics in Embryonic Vasculature Using Spectral Doppler Velocimetry," Anat. Rec. **292**(3), 311–319 (2009).
64. A. M. Davis, F. G. Rothenberg, N. Shepherd, and J. A. Izatt, "In vivo spectral domain optical coherence tomography volumetric imaging and spectral Doppler velocimetry of early stage embryonic chicken heart development," J. Opt. Soc. Am. A **25**(12), 3134–3143 (2008).
65. M. Zurauskas, A. Bradu, D. R. Ferguson, D. X. Hammer, and A. Podoleanu, "Closed loop tracked Doppler optical coherence tomography based heart monitor for the Drosophila melanogaster larvae," J. Biophotonics **9**(3), 246–252 (2016).
66. M. W. Jenkins, L. Peterson, S. Gu, M. Gargesha, D. L. Wilson, M. Watanabe, and A. M. Rollins, "Measuring hemodynamics in the developing heart tube with four-dimensional gated Doppler optical coherence tomography," J. Biomed. Opt. **15**(6), 066022 (2010).
67. A. Liu, X. Yin, L. Shi, P. Li, K. L. Thornburg, R. Wang, and S. Rugonyi, "Biomechanics of the Chick Embryonic Heart Outflow Tract at HH18 Using 4D Optical Coherence Tomography Imaging and Computational Modeling," PLoS One **7**(7), e40869 (2012).
68. M. Midgett, S. Goenezen, and S. Rugonyi, "Blood flow dynamics reflect degree of outflow tract banding in Hamburger–Hamilton stage 18 chicken embryos," J. R. Soc., Interface **11**(100), 20140643 (2014).
69. S. Gu, M. W. Jenkins, L. M. Peterson, Y. Q. Doughman, A. M. Rollins, and M. Watanabe, "Optical coherence tomography captures rapid hemodynamic responses to acute hypoxia in the cardiovascular system of early embryos," Dev. Dyn. **241**(3), 534–544 (2012).
70. B. A. Filas, I. R. Efimov, and L. A. Taber, "Optical Coherence Tomography as a Tool for Measuring Morphogenetic Deformation of the Looping Heart," Anat. Rec. **290**(9), 1057–1068 (2007).
71. L. Peng, L. Aiping, S. Liang, Y. Xin, R. Sandra, and K. W. Ruikang, "Assessment of strain and strain rate in embryonic chick heart in vivo using tissue Doppler optical coherence tomography," Phys. Med. Biol. **56**(22), 7081–7092 (2011).
72. Z. Ma, S. Dou, Y. Zhao, C. Guo, J. Liu, Q. Wang, T. Xu, R. K. Wang, and Y. Wang, "In vivo assessment of wall strain in embryonic chick heart by spectral domain optical coherence tomography," Appl. Opt. **54**(31), 9253–9257 (2015).
73. L. M. Peterson, M. W. Jenkins, S. Gu, L. Barwick, M. Watanabe, and A. M. Rollins, "4D shear stress maps of the developing heart using Doppler optical coherence tomography," Biomed. Opt. Express **3**(11), 3022–3032 (2012).
74. A. Liu, A. Nickerson, A. Troyer, X. Yin, R. Cary, K. Thornburg, R. Wang, and S. Rugonyi, "Quantifying blood flow and wall shear stresses in the outflow tract of chick embryonic hearts," Comput. Struct. **89**(11-12), 855–867 (2011).
75. Z. Y. G. Ko, K. Mehta, M. Jamil, C. H. Yap, and N. Chen, "A method to study the hemodynamics of chicken embryo's aortic arches using optical coherence tomography," J. Biophotonics **10**(3), 353–359 (2017).
76. S. Wang and K. V. Larin, "Optical coherence elastography for tissue characterization: a review," J. Biophotonics **8**(4), 279–302 (2015).
77. K. V. Larin and D. D. Sampson, "Optical coherence elastography - OCT at work in tissue biomechanics [Invited]," Biomed. Opt. Express **8**(2), 1172–1202 (2017).
78. L. Shi, S. Goenezen, S. Haller, M. T. Hinds, K. L. Thornburg, and S. Rugonyi, "Alterations in pulse wave propagation reflect the degree of outflow tract banding in HH18 chicken embryos," Am. J. Physiol-Heart. C. **305**(3), H386–H396 (2013).
79. P. Li and R. K. Wang, "Optical coherence tomography provides an ability to assess mechanical property of cardiac wall of developing outflow tract in embryonic heart in vivo," J. Biomed. Opt. **17**(12), 120502 (2012).
80. V. K. Chivukula, S. Goenezen, A. Liu, and S. Rugonyi, "Effect of Outflow Tract Banding on Embryonic Cardiac Hemodynamics," J. Cardiovasc. Dev. Dis. **3**(1), 1 (2016).

Biomedical Optics EXPRESS

81. M. Midgett, V. K. Chivukula, C. Dorn, S. Wallace, and S. Rugonyi, "Blood flow through the embryonic heart outflow tract during cardiac looping in HH13–HH18 chicken embryos," J. R. Soc., Interface **12**(111), 20150652 (2015).
82. K. Courchaine, M. J. Gray, K. Beel, K. Thornburg, and S. Rugonyi, "4-D Computational Modeling of Cardiac Outflow Tract Hemodynamics over Looping Developmental Stages in Chicken Embryos," J. Cardiovasc. Dev. Dis. **6**(1), 11 (2019).
83. L. M. Peterson, S. Gu, G. Karunamuni, M. W. Jenkins, M. Watanabe, and A. M. Rollins, "Embryonic aortic arch hemodynamics are a functional biomarker for ethanol-induced congenital heart defects [Invited]," Biomed. Opt. Express **8**(3), 1823–1837 (2017).
84. A. D. Aguirre, C. Zhou, H.-C. Lee, O. O. Ahsen, and J. G. Fujimoto, "Optical Coherence Microscopy," in *Optical Coherence Tomography: Technology and Applications*, W. Drexler and J. G. Fujimoto, eds. (Springer International Publishing, Cham, 2015), pp. 865–911.
85. K. Karnowski, A. Ajduk, B. Wieloch, S. Tamborski, K. Krawiec, M. Wojtkowski, and M. Szkulmowski, "Optical coherence microscopy as a novel, non-invasive method for the 4D live imaging of early mammalian embryos," Sci. Rep. **7**(1), 4165 (2017).
86. E. L. Moore, S. Wang, and I. V. Larina, "Staging mouse preimplantation development in vivo using optical coherence microscopy," J. Biophotonics **12**(5), e201800364 (2019).
87. L. Duan, X. Qin, Y. He, X. Sang, J. Pan, T. Xu, J. Men, R. E. Tanzi, A. Li, Y. Ma, and C. Zhou, "Segmentation of Drosophila heart in optical coherence microscopy images using convolutional neural networks," J. Biophotonics **11**(12), e201800146 (2018).
88. V. J. Srinivasan, H. Radhakrishnan, J. Y. Jiang, S. Barry, and A. E. Cable, "Optical coherence microscopy for deep tissue imaging of the cerebral cortex with intrinsic contrast," Opt. Express **20**(3), 2220–2239 (2012).
89. Z. Movasaghi, S. Rehman, and I. U. Rehman, "Raman Spectroscopy of Biological Tissues," Appl. Spectrosc. Rev. **42**(5), 493–541 (2007).
90. L. Opilik, T. Schmid, and R. Zenobi, "Modern Raman Imaging: Vibrational Spectroscopy on the Micrometer and Nanometer Scales," Annu. Rev. Anal. Chem. **6**(1), 379–398 (2013).
91. K. Klein, A. M. Gigler, T. Aschenbrenner, R. Monetti, W. Bunk, F. Jamitzky, G. Morfill, R. W. Stark, and J. Schlegel, "Label-Free Live-Cell Imaging with Confocal Raman Microscopy," Biophys. J. **102**(2), 360–368 (2012).
92. W. Dou, D. Zhang, Y. Jung, J.-X. Cheng, and D. M. Umulis, "Label-Free Imaging of Lipid-Droplet Intracellular Motion in Early Drosophila Embryos Using Femtosecond-Stimulated Raman Loss Microscopy," Biophys. J. **102**(7), 1666–1675 (2012).
93. M. J. Nakamura, K. Hotta, and K. Oka, "Raman Spectroscopic Imaging of the Whole Ciona intestinalis Embryo during Development," PLoS One **8**(8), e71739 (2013).
94. J. Bradley, I. Pope, F. Masia, R. Sanusi, W. Langbein, K. Swann, and P. Borri, "Quantitative imaging of lipids in live mouse oocytes and early embryos using CARS microscopy," Development **143**(12), 2238–2247 (2016).
95. J.-X. Cheng, "Coherent anti-Stokes Raman scattering microscopy," Appl. Spectrosc. **61**(9), 197A–208A (2007).
96. J. Ding, T. Xu, X. Tan, H. Jin, J. Shao, and H. Li, "Raman spectrum: A potential biomarker for embryo assessment during in vitro fertilization," Exp. Ther. Med. **13**(5), 1789–1792 (2017).
97. X. Dou, Y. Zhao, M. Li, Q. Chen, and Y. Yamaguchi, "Raman imaging diagnosis of the early stage differentiation of mouse embryonic stem cell (mESC)," Spectrochim. Acta, Part A **224**, 117438 (2020).
98. E. Perevedentseva, A. Krivokharchenko, A. V. Karmenyan, H.-H. Chang, and C.-L. Cheng, "Raman spectroscopy on live mouse early embryo while it continues to develop into blastocyst in vitro," Sci. Rep. **9**(1), 6636 (2019).
99. Z. Meng, A. J. Traverso, C. W. Ballmann, M. A. Troyanova-Wood, and V. V. Yakovlev, "Seeing cells in a new light: a renaissance of Brillouin spectroscopy," Adv. Opt. Photonics **8**(2), 300–327 (2016).
100. F. Palombo and D. Fioretto, "Brillouin Light Scattering: Applications in Biomedical Sciences," Chem. Rev. **119**(13), 7833–7847 (2019).
101. K. J. Koski and J. L. Yarger, "Brillouin imaging," Appl. Phys. Lett. **87**(6), 061903 (2005).
102. G. Scarcelli and S. H. Yun, "Confocal Brillouin microscopy for three-dimensional mechanical imaging," Nat. Photonics **2**(1), 39–43 (2008).
103. G. Scarcelli, W. J. Polacheck, H. T. Nia, K. Patel, A. J. Grodzinsky, R. D. Kamm, and S. H. Yun, "Noncontact three-dimensional mapping of intracellular hydromechanical properties by Brillouin microscopy," Nat. Methods **12**(12), 1132–1134 (2015).
104. G. Scarcelli, P. Kim, and S. H. Yun, "In vivo measurement of age-related stiffening in the crystalline lens by Brillouin optical microscopy," Biophys. J. **101**(6), 1539–1545 (2011).
105. G. Scarcelli, R. Pineda, and S. H. Yun, "Brillouin optical microscopy for corneal biomechanics," Invest. Ophthalmol. Visual Sci. **53**(1), 185–190 (2012).
106. R. Raghunathan, J. Zhang, C. Wu, J. Rippy, M. Singh, K. V. Larin, and G. Scarcelli, "Evaluating biomechanical properties of murine embryos using Brillouin microscopy and optical coherence tomography," J. Biomed. Opt. **22**(08), 1–6 (2017).
107. J. Zhang, R. Raghunathan, J. Rippy, C. Wu, R. H. Finnell, K. V. Larin, and G. Scarcelli, "Tissue biomechanics during cranial neural tube closure measured by Brillouin microscopy and optical coherence tomography," Birth Defects Res. **111**(14), 991–998 (2019).

Biomedical Optics EXPRESS

108. R. Schlüßler, S. Möllmert, S. Abuhattum, G. Cojoc, P. Müller, K. Kim, C. Möckel, C. Zimmermann, J. Czarske, and J. Guck, "Mechanical Mapping of Spinal Cord Growth and Repair in Living Zebrafish Larvae by Brillouin Imaging," Biophys. J. **115**(5), 911–923 (2018).
109. S. Majkut, T. Idema, J. Swift, C. Krieger, A. Liu, and D. E. Discher, "Heart-specific stiffening in early embryos parallels matrix and myosin expression to optimize beating," Curr. Biol. **23**(23), 2434–2439 (2013).
110. X. Chen, O. Nadiarynkh, S. Plotnikov, and P. J. Campagnola, "Second harmonic generation microscopy for quantitative analysis of collagen fibrillar structure," Nat. Protoc. **7**(4), 654–669 (2012).
111. B. Weigelin, G.-J. Bakker, and P. Friedl, "Third harmonic generation microscopy of cells and tissue organization," J. Cell Sci. **129**(2), 245–255 (2016).
112. P. J. Campagnola, A. C. Millard, M. Terasaki, P. E. Hoppe, C. J. Malone, and W. A. Mohler, "Three-dimensional high-resolution second-harmonic generation imaging of endogenous structural proteins in biological tissues," Biophys. J. **82**(1), 493–508 (2002).
113. P. J. Campagnola and L. M. Loew, "Second-harmonic imaging microscopy for visualizing biomolecular arrays in cells, tissues and organisms," Nat. Biotechnol. **21**(11), 1356–1360 (2003).
114. V. Nucciotti, C. Stringari, L. Sacconi, F. Vanzi, L. Fusi, M. Linari, G. Piazzesi, V. Lombardi, and F. S. Pavone, "Probing myosin structural conformation in vivo by second-harmonic generation microscopy," Proc. Natl. Acad. Sci. **107**(17), 7763–7768 (2010).
115. C.-Y. Lin, V. A. Hovhannisyan, J.-T. Wu, C.-W. Lin, J.-H. Chen, S.-J. Lin, and C.-Y. Dong, "Label-free imaging of Drosophila larva by multiphoton autofluorescence and second harmonic generation microscopy," J. Biomed. Opt. **13**(5), 050502 (2008).
116. S. Bancelin, C. A. Couture, M. Pinsard, M. Rivard, P. Drapeau, and F. Légaré, "Probing microtubules polarity in mitotic spindles in situ using Interferometric Second Harmonic Generation Microscopy," Sci. Rep. **7**(1), 6758 (2017).
117. A. L. Lopez and I. V. Larina, "Second harmonic generation microscopy of early embryonic mouse hearts," Biomed. Opt. Express **10**(6), 2898–2908 (2019).
118. G. J. Tserevelakis, G. Filippidis, C. Fotakis, E. V. Megalou, and N. Tavemarakis, "Cell tracking in live Caenorhabditis elegans embryos via third harmonic generation imaging microscopy measurements," J. Biomed. Opt. **16**(4), 046019 (2011).
119. S. Dietzel, J. Pircher, A. K. Nekolla, M. Gull, A. W. Brändli, U. Pohl, and M. Rehberg, "Label-Free Determination of Hemodynamic Parameters in the Microcirculaton with Third Harmonic Generation Microscopy," PLoS One **9**(6), e99615 (2014).
120. C.-S. Hsieh, S.-U. Chen, Y.-W. Lee, Y.-S. Yang, and C.-K. Sun, "Higher harmonic generation microscopy of in vitro cultured mammal oocytes and embryos," Opt. Express **16**, 11574–11588 (2008).
121. N. Olivier, M. A. Luengo-Oroz, L. Duloquin, E. Faure, T. Savy, I. Veilleux, X. Solinas, D. Débarre, P. Bourgine, A. Santos, N. Peyriéras, and E. Beaurepaire, "Cell Lineage Reconstruction of Early Zebrafish Embryos Using Label-Free Nonlinear Microscopy," Science **329**(5994), 967–971 (2010).
122. A. Jesacher, A. Thayil, K. Grieve, D. Débarre, T. Watanabe, T. Wilson, S. Srinivas, and M. Booth, "Adaptive harmonic generation microscopy of mammalian embryos," Opt. Lett. **34**(20), 3154–3156 (2009).
123. T. Watanabe, A. Thayil, A. Jesacher, K. Grieve, D. Debarre, T. Wilson, M. Booth, and S. Srinivas, "Characterisation of the dynamic behaviour of lipid droplets in the early mouse embryo using adaptive harmonic generation microscopy," BMC Cell Biol. **11**(1), 38 (2010).
124. A. Thayil, T. Watanabe, A. Jesacher, T. Wilson, S. Srinivas, and M. Booth, "Long-term imaging of mouse embryos using adaptive harmonic generation microscopy," J. Biomed. Opt. **16**(4), 046018 (2011).
125. J. Sharpe, "Optical Projection Tomography," Annu. Rev. Biomed. Eng. **6**(1), 209–228 (2004).
126. L. Quintana and J. Sharpe, "Optical Projection Tomography of Vertebrate Embryo Development," Cold Spring Harbor Protocols 2011, pdb.top116 (2011).
127. N. Martínez-Abadías, R. Mateu Estivill, J. Sastre Tomas, S. Motch Perrine, M. Yoon, A. Robert-Moreno, J. Swoger, L. Russo, K. Kawasaki, J. Richtsmeier, and J. Sharpe, "Quantification of gene expression patterns to reveal the origins of abnormal morphogenesis," eLife **7**, e36405 (2018).
128. C. G. Arques, R. Doohan, J. Sharpe, and M. Torres, "Cell tracing reveals a dorsoventral lineage restriction plane in the mouse limb bud mesenchyme," Development **134**(20), 3713–3722 (2007).
129. A. Asayesh, J. Sharpe, R. P. Watson, J. Hecksher-Sørensen, N. D. Hastie, R. E. Hill, and U. Ahlgren, "Spleen versus pancreas: strict control of organ interrelationship revealed by analyses of Bapx1-/- mice," Genes Dev. **20**(16), 2208–2213 (2006).
130. S. Sarma, J. Kerwin, L. Puelles, M. Scott, T. Strachan, G. Feng, J. Sharpe, D. Davidson, R. Baldock, and S. Lindsay, "3D modelling, gene expression mapping and post-mapping image analysis in the developing human brain," Brain Res. Bull. **66**(4-6), 449–453 (2005).
131. J. Sharpe, "Optical projection tomography as a new tool for studying embryo anatomy," J. Anat. **202**(2), 175–181 (2003).
132. M. Singh, R. Raghunathan, V. Piazza, A. M. Davis-Loiacono, A. Cable, T. J. Vedakkan, T. Janecek, M. V. Frazier, A. Nair, C. Wu, I. V. Larina, M. E. Dickinson, and K. V. Larin, "Applicability, usability, and limitations of murine embryonic imaging with optical coherence tomography and optical projection tomography," Biomed. Opt. Express **7**(6), 2295–2310 (2016).

Biomedical Optics EXPRESS

133. J. Kerwin, M. Scott, J. Sharpe, L. Puelles, S. C. Robson, M. Martínez-de-la-Torre, J. L. Ferran, G. Feng, R. Baldock, T. Strachan, D. Davidson, and S. Lindsay, "3 dimensional modelling of early human brain development using optical projection tomography," BMC Neurosci. **5**(1), 27 (2004).
134. L. Quintana and J. Sharpe, "Preparation of Mouse Embryos for Optical Projection Tomography Imaging," Cold Spring Harbor Protocols 2011, pdb.prot5639 (2011).
135. M. Rieckher, U. J. Birk, H. Meyer, J. Ripoll, and N. Tavernarakis, "Microscopic Optical Projection Tomography In Vivo," PLoS One **6**(4), e18963 (2011).
136. T. Correia, N. Lockwood, S. Kumar, J. Yin, M.-C. Ramel, N. Andrews, M. Katan, L. Bugeon, M. J. Dallman, J. McGinty, P. Frankel, P. M. W. French, and S. Arridge, "Accelerated Optical Projection Tomography Applied to In Vivo Imaging of Zebrafish," PLoS One **10**(8), e0136213 (2015).
137. A. Arranz, D. Dong, S. Zhu, C. Savakis, J. Tian, and J. Ripoll, "In-vivo Optical Tomography of Small Scattering Specimens: time-lapse 3D imaging of the head eversion process in Drosophila melanogaster," Sci. Rep. **4**(1), 7325 (2015).
138. M. J. Boot, C. H. Westerberg, J. Sanz-Ezquerro, J. Cotterell, R. Schweitzer, M. Torres, and J. Sharpe, "In vitro whole-organ imaging: 4D quantification of growing mouse limb buds," Nat. Methods **5**(7), 609–612 (2008).
139. J.-F. Colas and J. Sharpe, "Live optical projection tomography," Organogenesis **5**(4), 211–216 (2009).
140. M. Xu and L. V. Wang, "Photoacoustic imaging in biomedicine," Rev. Sci. Instrum. **77**(4), 041101 (2006).
141. S. Manohar and D. Razansky, "Photoacoustics: a historical review," Adv. Opt. Photonics **8**(4), 586–617 (2016).
142. J. Yao and L. V. Wang, "Photoacoustic tomography: fundamentals, advances and prospects," Contrast Media Mol. Imaging **6**(5), 332–345 (2011).
143. J. Xia, J. Yao, and L. V. Wang, "Photoacoustic tomography: principles and advances," Prog. Electromagn. Res. **147**, 1–22 (2014).
144. L. V. Wang and S. Hu, "Photoacoustic Tomography: In Vivo Imaging from Organelles to Organs," Science **335**(6075), 1458–1462 (2012).
145. L. V. Wang and J. Yao, "A practical guide to photoacoustic tomography in the life sciences," Nat. Methods **13**(8), 627–638 (2016).
146. J. Laufer, F. C. Norris, J. O. Cleary, E. Z. Zhang, B. E. Treeby, B. T. Cox, S. P. Johnson, P. Scambler, M. F. Lythgoe, and P. C. Beard, "In vivo photoacoustic imaging of mouse embryos," J. Biomed. Opt. **17**(6), 061220 (2012).
147. C. L. Bayer, B. J. Wlodarczyk, R. H. Finnell, and S. Y. Emelianov, "Ultrasound-guided spectral photoacoustic imaging of hemoglobin oxygenation during development," Biomed. Opt. Express **8**(2), 757–763 (2017).
148. M. Liu, B. Maurer, B. Hermann, B. Zabihian, M. G. Sandrian, A. Unterhuber, B. Baumann, E. Z. Zhang, P. C. Beard, W. J. Weninger, and W. Drexler, "Dual modality optical coherence and whole-body photoacoustic tomography imaging of chick embryos in multiple development stages," Biomed. Opt. Express **5**(9), 3150–3159 (2014).
149. S. Ye, R. Yang, J. Xiong, K. K. Shung, Q. Zhou, C. Li, and Q. Ren, "Label-free imaging of zebrafish larvae in vivo by photoacoustic microscopy," Biomed. Opt. Express **3**(2), 360–365 (2012).
150. Q. Chen, T. Jin, W. Qi, X. Mo, and L. Xi, "Label-free photoacoustic imaging of the cardio-cerebrovascular development in the embryonic zebrafish," Biomed. Opt. Express **8**(4), 2359–2367 (2017).
151. M. J. Moore, S. El-Rass, Y. Xiao, Y. Wang, X.-Y. Wen, and M. C. Kolios, "Simultaneous ultra-high frequency photoacoustic microscopy and photoacoustic radiometry of zebrafish larvae in vivo," Photoacoustics **12**, 14–21 (2018).
152. J. Yang, L. Gong, X. Xu, P. Hai, Y. Shen, Y. Suzuki, and L. V. Wang, "Motionless volumetric photoacoustic microscopy with spatially invariant resolution," Nat. Commun. **8**(1), 780 (2017).
153. D.-K. Yao, R. Chen, K. Maslov, Q. Zhou, and L. V. Wang, "Optimal ultraviolet wavelength for in vivo photoacoustic imaging of cell nuclei," J. Biomed. Opt. **17**(5), 056004 (2012).
154. Z. Xu, Q. Zhu, and L. V. Wang, "In vivo photoacoustic tomography of mouse cerebral edema induced by cold injury," J. Biomed. Opt. **16**(6), 066020 (2011).
155. G. S. Sangha, E. H. Phillips, and C. J. Goergen, "In vivo photoacoustic lipid imaging in mice using the second near-infrared window," Biomed. Opt. Express **8**(2), 736–742 (2017).
156. T. Matthews, C. Zhang, D.-K. Yao, K. Maslov, and L. Wang, "Label-free photoacoustic microscopy of peripheral nerves," J. Biomed. Opt. **19**(1), 016004 (2014).
157. P. Wang, P. Wang, H.-W. Wang, and J.-X. Cheng, "Mapping lipid and collagen by multispectral photoacoustic imaging of chemical bond vibration," J. Biomed. Opt. **17**(9), 0960101 (2012).
158. Y. Park, C. Depeursinge, and G. Popescu, "Quantitative phase imaging in biomedicine," Nat. Photonics **12**(10), 578–589 (2018).
159. M. Mir, T. Kim, A. Majumder, M. Xiang, R. Wang, S. C. Liu, M. U. Gillette, S. Stice, and G. Popescu, "Label-Free Characterization of Emerging Human Neuronal Networks," Sci. Rep. **4**(1), 4434 (2015).
160. S. Sridharan, M. Mir, and G. Popescu, "Simultaneous optical measurements of cell motility and growth," Biomed. Opt. Express **2**(10), 2815–2820 (2011).
161. Y. Park, C. A. Best, K. Badizadegan, R. R. Dasari, M. S. Feld, T. Kuriabova, M. L. Henle, A. J. Levine, and G. Popescu, "Measurement of red blood cell mechanics during morphological changes," Proc. Natl. Acad. Sci. **107**(15), 6731–6736 (2010).
162. T. H. Nguyen, M. E. Kandel, M. Rubessa, M. B. Wheeler, and G. Popescu, "Gradient light interference microscopy for 3D imaging of unlabeled specimens," Nat. Commun. **8**(1), 210 (2017).

Biomedical Optics EXPRESS

163. T. Mammoto and D. E. Ingber, "Mechanical control of tissue and organ development," Development **137**(9), 1407–1420 (2010).
164. C. P. Toseland, "Fluorescent labeling and modification of proteins," J Chem Biol **6**(3), 85–95 (2013).
165. B.-C. Chen, W. R. Legant, K. Wang, L. Shao, D. E. Milkie, M. W. Davidson, C. Janetopoulos, X. S. Wu, J. A. Hammer, Z. Liu, B. P. English, Y. Mimori-Kiyosue, D. P. Romero, A. T. Ritter, J. Lippincott-Schwartz, L. Fritz-Laylin, R. D. Mullins, D. M. Mitchell, J. N. Bembenek, A.-C. Reymann, R. Böhme, S. W. Grill, J. T. Wang, G. Seydoux, U. S. Tulu, D. P. Kiehart, and E. Betzig, "Lattice light-sheet microscopy: Imaging molecules to embryos at high spatiotemporal resolution," Science **346**(6208), 1257998 (2014).
166. L. A. Royer, W. C. Lemon, R. K. Chhetri, Y. Wan, M. Coleman, E. W. Myers, and P. J. Keller, "Adaptive light-sheet microscopy for long-term, high-resolution imaging in living organisms," Nat. Biotechnol. **34**(12), 1267–1278 (2016).
167. V. Voleti, K. B. Patel, W. Li, C. Perez Campos, S. Bharadwaj, H. Yu, C. Ford, M. J. Casper, R. W. Yan, W. Liang, C. Wen, K. D. Kimura, K. L. Targoff, and E. M. C. Hillman, "Real-time volumetric microscopy of in vivo dynamics and large-scale samples with SCAPE 2.0," Nat. Methods **16**(10), 1054–1062 (2019).
168. C. Wu, H. Le, S. Ran, M. Singh, I. V. Larina, D. Mayerich, M. E. Dickinson, and K. V. Larin, "Comparison and combination of rotational imaging optical coherence tomography and selective plane illumination microscopy for embryonic study," Biomed. Opt. Express **8**(10), 4629 (2017).
169. J. Brunker, J. Yao, J. Laufer, and S. E. Bohndiek, "Photoacoustic imaging using genetically encoded reporters: a review," J. Biomed. Opt. **22**(7), 070901 (2017).
170. C. Yang, "Molecular contrast optical coherence tomography: a review," Photochem. Photobiol. **81**(2), 215–237 (2005).
171. D. Razansky, M. Distel, C. Vinegoni, R. Ma, N. Perrimon, R. W. Köster, and V. Ntziachristos, "Multispectral opto-acoustic tomography of deep-seated fluorescent proteins in vivo," Nat. Photonics **3**(7), 412–417 (2009).
172. J. Yao, A. A. Kaberniuk, L. Li, D. M. Shcherbakova, R. Zhang, L. Wang, G. Li, V. V. Verkhusha, and L. V. Wang, "Multiscale photoacoustic tomography using reversibly switchable bacterial phytochrome as a near-infrared photochromic probe," Nat. Methods **13**(1), 67–73 (2016).
173. D. Razansky, C. Vinegoni, and V. Ntziachristos, "Multispectral photoacoustic imaging of fluorochromes in small animals," Opt. Lett. **32**(19), 2891–2893 (2007).
174. W. Kim and B. E. Applegate, "In vivo molecular contrast OCT imaging of methylene blue," Opt. Lett. **40**(7), 1426–1429 (2015).
175. A. Desgrange, J. Lokmer, C. Marchiol, L. Houyel, and S. M. Meilhac, "Standardised imaging pipeline for phenotyping mouse laterality defects and associated heart malformations, at multiple scales and multiple stages," Dis. Models Mech. **12**(7), dmm038356 (2019).
176. S. You, H. Tu, E. J. Chaney, Y. Sun, Y. Zhao, A. J. Bower, Y.-Z. Liu, M. Marjanovic, S. Sinha, Y. Pu, and S. A. Boppart, "Intravital imaging by simultaneous label-free autofluorescence-multiharmonic microscopy," Nat. Commun. **9**(1), 2125 (2018).
177. A. Alex, A. Li, R. E. Tanzi, and C. Zhou, "Optogenetic pacing in Drosophila melanogaster," Sci. Adv. **1**(9), e1500639 (2015).
178. J. A. Bolker, "Model systems in developmental biology," BioEssays **17**(5), 451–455 (1995).
179. K. V. Anderson and P. W. Ingham, "The transformation of the model organism: a decade of developmental genetics," Nat. Genet. **33**(S3), 285–293 (2003).
180. M. D. Garcia, R. S. Udan, A.-K. Hadjantonakis, and M. E. Dickinson, "Preparation of Postimplantation Mouse Embryos for Imaging," Cold Spring Harbor Protocols 2011, pdb.prot5594 (2011).
181. M. E. Dickinson, A. M. Flenniken, X. Ji, L. Teboul, M. D. Wong, J. K. White, T. F. Meehan, W. J. Weninger, H. Westerberg, H. Adissu, C. N. Baker, L. Bower, J. M. Brown, L. B. Caddle, F. Chiani, D. Clary, J. Cleak, M. J. Daly, J. M. Denegre, B. Doe, M. E. Dolan, S. M. Edie, H. Fuchs, V. Gailus-Durner, A. Galli, A. Gambadoro, J. Gallegos, S. Guo, N. R. Horner, C.-W. Hsu, S. J. Johnson, S. Kalaga, L. C. Keith, L. Lanoue, T. N. Lawson, M. Lek, M. Mark, S. Marschall, J. Mason, M. L. McElwee, S. Newbigging, L. M. J. Nutter, K. A. Peterson, R. Ramirez-Solis, D. J. Rowland, E. Ryder, K. E. Samocha, J. R. Seavitt, M. Selloum, Z. Szoke-Kovacs, M. Tamura, A. G. Trainor, I. Tudose, S. Wakana, J. Warren, O. Wendling, D. B. West, L. Wong, A. Yoshiki, C. International Mouse Phenotyping, L. Jackson, I. C. d. l. S. Infrastructure Nationale Phenomin, L. Charles River, M. R. C. Harwell, P. Toronto Centre for, I. Wellcome Trust Sanger, R. B. Center, D. G. MacArthur, G. P. Tocchini-Valentini, X. Gao, P. Flicek, A. Bradley, W. C. Skarnes, M. J. Justice, H. E. Parkinson, M. Moore, S. Wells, R. E. Braun, K. L. Svenson, M. H. de Angelis, Y. Herault, T. Mohun, A.-M. Mallon, R. M. Henkelman, S. D. M. Brown, D. J. Adams, K. C. K. Lloyd, C. McKerlie, A. L. Beaudet, M. Bućan, and S. A. Murray, "High-throughput discovery of novel developmental phenotypes," Nature **537**(7621), 508–514 (2016).
182. D. B. West, R. K. Pasumarthi, B. Baridon, E. Djan, A. Trainor, S. M. Griffey, E. K. Engelhard, J. Rapp, B. Li, P. J. d. Jong, and K. C. K. Lloyd, "A lacZ reporter gene expression atlas for 313 adult KOMP mutant mouse lines," Genome Res. **25**(4), 598–607 (2015).
183. L. Li, L. Zhu, C. Ma, L. Lin, J. Yao, L. Wang, K. Maslov, R. Zhang, W. Chen, J. Shi, and L. V. Wang, "Single-impulse Panoramic Photoacoustic Computed Tomography of Small-animal Whole-body Dynamics at High Spatiotemporal Resolution," Nat. Biomed. Eng. **1**(5), 0071 (2017).
184. D. Shen, G. Wu, and H.-I. Suk, "Deep Learning in Medical Image Analysis," Annu. Rev. Biomed. Eng. **19**(1), 221–248 (2017).

Biomedical Optics EXPRESS

185. A. Moorman, S. Webb, N. A. Brown, W. Lamers, and R. H. Anderson, "Development of the heart: (1) formation of the cardiac chambers and arterial trunks," Br. Heart J. **89**(7), 806–814 (2003).
186. S. Goenezen, M. Y. Rennie, and S. Rugonyi, "Biomechanics of early cardiac development," Biomech. Model. Mechanobiol. **11**(8), 1187–1204 (2012).
187. J. Männer, A. Wessel, and T. M. Yelbuz, "How does the tubular embryonic heart work? Looking for the physical mechanism generating unidirectional blood flow in the valveless embryonic heart tube," Dev. Dyn. **239**(4), 1035–1046 (2010).
188. G. H. Karunamuni, S. Gu, M. R. Ford, L. M. Peterson, P. Ma, Y. T. Wang, A. M. Rollins, M. W. Jenkins, and M. Watanabe, "Capturing structure and function in an embryonic heart with biophotonic tools," Front. Physiol. **5**, 351 (2014).
189. A. S. Forouhar, M. Liebling, A. Hickerson, A. Nasiraei-Moghaddam, H. J. Tsai, J. R. Hove, S. E. Fraser, M. E. Dickinson, and M. Gharib, "The embryonic vertebrate heart tube is a dynamic suction pump," Science **312**(5774), 751–753 (2006).
190. M. Liebling, A. S. Forouhar, R. Wolleschensky, B. Zimmermann, R. Ankerhold, S. E. Fraser, M. Gharib, and M. E. Dickinson, "Rapid three-dimensional imaging and analysis of the beating embryonic heart reveals functional changes during development," Dev. Dyn. **235**(11), 2940–2948 (2006).
191. M. Lockhart, E. Wirrig, A. Phelps, and A. Wessels, "Extracellular matrix and heart development," Birth Defects Res., Part A **91**(6), 535–550 (2011).
192. A. J. Copp and N. D. Greene, "Genetics and development of neural tube defects," J. Pathol. **220**, 217–230 (2009).
193. R. Raghunathan, C. Wu, M. Singh, C.-H. Liu, R. C. Miranda, and K. V. Larin, "Evaluating the effects of maternal alcohol consumption on murine fetal brain vasculature using optical coherence tomography," J. Biophotonics **11**(5), e201700238 (2018).
194. R. Raghunathan, C.-H. Liu, A. Kouka, M. Singh, R. C. Miranda, and K. V. Larin, "Assessing the Acute Effects of Prenatal Synthetic Cannabinoid Exposure on Murine Fetal Brain Vasculature Using Optical Coherence Tomography," J. Biophotonics **12**, e201900050 (2019).
195. E. Nikolopoulou, G. L. Galea, A. Rolo, N. D. E. Greene, and A. J. Copp, "Neural tube closure: cellular, molecular and biomechanical mechanisms," Development **144**(4), 552–566 (2017).
196. G. L. Galea, Y.-J. Cho, G. Galea, M. A. Molè, A. Rolo, D. Savery, D. Moulding, L. H. Culshaw, E. Nikolopoulou, N. D. E. Greene, and A. J. Copp, "Biomechanical coupling facilitates spinal neural tube closure in mouse embryos," Proc. Natl. Acad. Sci. **114**(20), 5177–5182 (2017).
197. R. Sturmey, A. Reis, H. Leese, and T. McEvoy, "Role of Fatty Acids in Energy Provision During Oocyte Maturation and Early Embryo Development," Reprod. Domest. Anim. **44**, 50–58 (2009).
198. R. Aizawa, M. Ibayashi, T. Tatsumi, A. Yamamoto, T. Kokubo, N. Miyasaka, K. Sato, S. Ikeda, N. Minami, and S. Tsukamoto, "Synthesis and maintenance of lipid droplets are essential for mouse preimplantation embryonic development," Development **146**(22), dev181925 (2019).